An integrated systems-level model of the toxicity of brevetoxin based on high-resolution magic-angle spinning nuclear magnetic resonance (HRMAS NMR) metabolic profiling of zebrafish embryos

Annunziato, M.; Eeza, M.N.H.; Bashirova, N.; Lawson, A.; Matysik, J.; Benetti, D.; ... ; Berry, J.P.

Science of the Total Environment 803 (2022) 149858

Contents lists available at ScienceDirect

Science of the Total Environment

journal homepage: www.elsevier.com/locate/scitotenv

An integrated systems-level model of the toxicity of brevetoxin based on high-resolution magic-angle spinning nuclear magnetic resonance (HRMAS NMR) metabolic profiling of zebrafish embryos

Mark Annunziato [a], Muhamed N.H. Eeza [b,c], Narmin Bashirova [b,c], Ariel Lawson [a], Jörg Matysik [c], Daniel Benetti [d], Martin Grosell [d], John D. Stieglitz [d], A. Alia [b,e,*], John P. Berry [a,f,**]

[a] Institute of Environment, Department of Chemistry and Biochemistry, Florida International University, 3000 NE 151st Street, North Miami, FL 33181, USA
[b] Institute of Medical Physics and Biophysics, University of Leipzig, Leipzig, Germany
[c] Institute for Analytical Chemistry, University of Leipzig, Leipzig, Germany
[d] Rosenstiel School of Marine and Atmospheric Sciences, University of Miami, Miami, FL, USA
[e] Leiden Institute of Chemistry, Leiden University, 2333 Leiden, the Netherlands
[f] Biomolecular Science Institute, Florida International University, 11200 SW 8th Street, Miami, FL 33199, USA

HIGHLIGHTS

- PbTx-2 is toxic to embryos of both zebrafish and mahi-mahi.
- Embryotoxicity was observed at environmentally relevant concentrations.
- PbTx-2 altered levels of metabolites associated with neurotoxicity and energy metabolism.
- An integrated *systems-level* model of toxicity of PbTx-2 was enabled by metabolic profiles.
- Metabolic profiles suggest potential biomarkers for environmental monitoring.

GRAPHICAL ABSTRACT

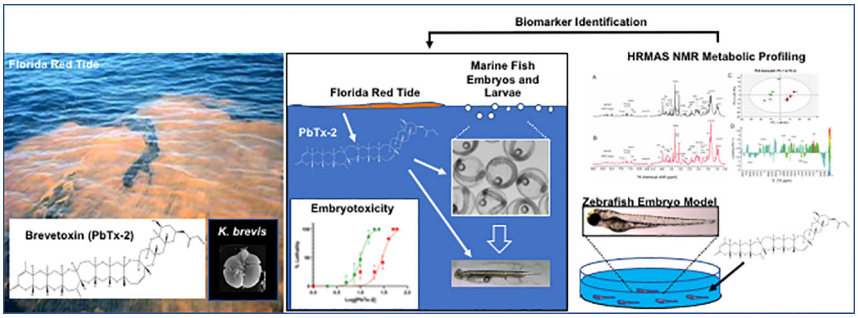

ARTICLE INFO

Article history:
Received 9 April 2021
Received in revised form 18 August 2021
Accepted 19 August 2021
Available online 22 August 2021

Editor: Lotfi Aleya

Keywords:
Brevetoxin
Zebrafish
Mahi-mahi
Metabolomics
Neurotoxicity
HRMAS NMR

ABSTRACT

Brevetoxins (PbTx) are a well-recognized group of neurotoxins associated with harmful algal blooms, and specifically recurrent "Florida Red Tides," in marine waters that are linked to impacts on both human and ecosystem health including well-documented "fish kills" and marine mammal mortalities in affected coastal waters. Understanding mechanisms and pathways of PbTx toxicity enables identification of relevant *biomarkers* to better understand these environmental impacts, and improve monitoring efforts, in relation to this toxin. Toward a *systems-level* understanding of toxicity, and identification of potential biomarkers, high-resolution magic angle spinning nuclear magnetic resonance (HRMAS NMR) was utilized for metabolic profiling of zebrafish (*Danio rerio*) embryos, as an established toxicological model, exposed to PbTx-2 (the most common congener in marine waters). Metabolomics studies were, furthermore, complemented by an assessment of the toxicity of PbTx-2 in embryonic stages of zebrafish and mahi-mahi (*Coryphaena hippurus*), the latter representing an ecologically and geographically relevant marine species of fish, which identified acute embryotoxicity at environmentally relevant (i.e., parts-per-billion) concentrations in both species. HRMAS NMR analysis of intact zebrafish embryos exposed to sub-lethal concentrations of PbTx-2 afforded well-resolved spectra, and in turn, identification of 38 metabolites of which 28 were found to be significantly altered, relative to controls. Metabolites altered by

* Correspondence to: A. Alia, Institute of Medical Physics and Biophysics, University of Leipzig, Leipzig, Germany.
** Correspondence to: J.P. Berry, Institute of Environment, Department of Chemistry and Biochemistry, Florida International University, 3000 NE 151st Street, North Miami, FL 33181, USA.
E-mail addresses: Alia.AliaMatysik@medizin.uni-leipzig.de (A. Alia), berryj@fiu.edu (J.P. Berry).

https://doi.org/10.1016/j.scitotenv.2021.149858

PbTx-2 exposure specifically included those associated with (1) neuronal excitotoxicity, as well as associated neural homeostasis, and (2) interrelated pathways of carbohydrate and energy metabolism. Metabolomics studies, thereby, enabled a systems-level model of PbTx toxicity which integrated multiple metabolic, molecular and cellular pathways, in relation to environmentally relevant concentrations of the toxin, providing insight to not only targets and mechanisms, but potential biomarkers pertinent to environmental risk assessment and monitoring strategies.

1. Introduction

Brevetoxins (PbTx) are a group of neurotoxic metabolites primarily produced by the marine dinoflagellate, *Karenia brevis*, in association with algal blooms (i.e., "Red Tide") in the Gulf of Mexico, and along the southeastern coast of Florida where they have been linked to intoxications of marine animals, and adverse effects on human health (Baden, 1989; Landsberg, 2002; Kirkpatrick et al., 2006; Watkins et al., 2008). Structurally, brevetoxins are trans-fused cyclic polyethers which are separated into two types, Type A and Type B, with the major congeners being PbTx-1 and PbTx-2, respectively, and the latter being the most abundant form found in seawater (Pierce et al., 2010). Red Tide blooms are typically found to produce cell-free concentrations of PbTx variants in parts-per-billion to parts-per-million range (Buck and Pierce, 1989; Pierce et al., 2003; Pierce et al., 2005). Notably, however, it has been previously shown that PbTx may further concentrate at the sea surface, and uppermost layers of the marine water column, potentiating both aerosolization of the toxin (Pierce et al., 2003), and possible exposure of buoyant early-life stages of marine fish and invertebrates which are localized to these upper layers (Rumbold and Snedaker, 1999). Human exposure to PbTx can result from aerosolization of toxin-containing water, as well as ingestion of contaminated shellfish. In the latter case, foodborne exposure is associated with Neurotoxic Shellfish Poisoning (NSP) which is characterized by a range of both gastrointestinal and neurological symptoms (Watkins et al., 2008), whereas aerosolized PbTx has been largely linked to respiratory distress and related symptomology (e.g., burning of eyes and throat; Kirkpatrick et al., 2006). Blooms of PbTx-producing *K. brevis* are, however, most frequently associated with adverse effects on marine animal populations including mass mortality of fish (i.e., "fish kills"), and marine mammals including dolphins and manatees (Landsberg, 2002; Fire et al., 2015; Driggers et al., 2016), and numerous studies have, indeed, documented toxicity to fish (Rein et al., 1994; Kimm-Brinson and Ramsdell, 2001; Lu and Tomchik, 2002; Colman and Ramsdell, 2003; Choich et al., 2004; Bourdelais et al., 2005; Salierno et al., 2006; Bakke and Horsberg, 2007; Nam et al., 2010; Tian et al., 2011; Dorantes-Aranda et al., 2015; Lydon et al., 2020). Accordingly, fish (and other marine animals) represent potential "sentinel species" for understanding the role of PbTx toxicity in these ecosystems (i.e., risk assessment), as well as environmental monitoring strategies.

Identification of biochemical, molecular and cellular targets - as potential *biomarkers* - of PbTx is a key strategy (as it has been, likewise, recognized for a wide range of toxicants; Hagger et al., 2006) to improve environmental risk assessment and monitoring. And while details of the primary molecular targets of PbTx, particularly in relation to its recognized neurotoxic (i.e., "excitotoxic") activity, have been well investigated, a holistic view of the pathways of toxicity, in this regard, has remained elusive. The neurotoxicity of PbTx has been generally well-established to result primarily from binding to voltage-gated sodium channels (VGSC) causing the prolonged opening of the sodium channel, and specifically, the inability to inactivate the open channel leading to sustained depolarization of neural cells (Lombet et al., 1987; Trainer et al., 1993; Berman and Murray, 1999). Depolarization, as a result of VGSC binding, in turn, leads to several downstream neurochemical effects such as the enhanced release of glutamate leading to overstimulation of NMDA receptors (NMDAR), and an uncontrolled influx of Ca^{2+} into postsynaptic cells. While VGSC-binding has been rather clearly elucidated as a target for neurotoxic effects, the role of this mechanism in other symptomology including, for example, respiratory distress and associated effects remains, however, unclear (Kirkpatrick et al., 2004). Previous studies (e.g., Dechraoui et al., 1999) have, likewise, observed that the acute toxicity of PbTx in animal (i.e., mouse) models is not entirely correlated to their affinity for the VGSC, and have, thus, suggested that there are possibly other mechanisms that may contribute to toxicity. And recent studies, in fact, have pointed to other potentially relevant modes of action including, for example, oxidative stress via apparent thioredoxin reductase-based mechanisms (Tuladhar et al., 2019), and effects on the immune system (Pierre et al., 2018).

Given the apparent multimodal and multifaceted toxicity of PbTx (and, indeed, that of many other toxins), it is important to gain a better understanding of toxicity beyond conventional molecular toxicology models which typically focus on selected endpoints, and move toward a *systems biology* approach to better understand the holistic and integrated effects at the cellular and/or whole organism level. This approach has been increasingly realized, in particular, through various "omics" studies. A handful of attempts have, indeed, been made to understand the toxicity of PbTx from such an approach. Tian et al. (2011), for example, utilized matrix-assisted laser desorption/ionization tandem time-of-flight mass spectrometry (MALDI-TOF/TOF MS) for ex vivo analysis of brain extracts from the teleost fish model, medaka (*Oryzias latipes*), to study proteomic modifications after exposure to PbTx-1, and found that numerous proteins connected to Ca^{2+} ion binding were altered, alongside down-regulation of several proteins involved in cell protection. More recently, Yau et al. (2019) investigated changes in the neurotransmitter profiles of medaka exposed to PbTx-1 by LC-MS/MS analysis of brain extracts, and identified changes in several metabolites associated with VGSC and activation of NMDAR, as well as cholinergic neurotransmission. Notably, these studies (and the present) focus on fish as ecologically relevant receptors of PbTx, and thus, have direct relevance to ecotoxicology and other environmental assessments (e.g., risk assessment, monitoring)

One metabolomics approach which has recently shown considerable promise, in this regard, has been the use of nuclear magnetic resonance (NMR), and particularly *high-resolution magic angle spinning* (HRMAS) NMR, which enables metabolic profiling of intact cells, tissues and whole organisms (Gogiashvili et al., 2019; Lucas-Torres and Wong, 2020). Briefly, stated HRMAS NMR employs spinning of samples at the so-called "magic angle" ($\theta_m = 54.74°$) relative to the magnetic field, as well as specialized field gradients, to minimize or eliminate interactions including anisotropic, dipolar and quadrupolar effects, enabling highly resolved spectra of compound mixtures in complex matrices. In the context of metabolomics, this approach allows diverse metabolic profiles to be resolved, quantified and identified within complex biological matrices including intact organisms: most recently, this approach has been specifically employed to investigate modulation of metabolic profiles by various toxicants in early life stages, i.e., embryos and larvae, of the zebrafish (*Danio rerio*). Zebrafish embryo and larval stages have, in general, been well established as a toxicological model, and toxicity assays based on this model system have been developed and applied to the assessment of a wide range of

environmental toxicants including biotoxins and environmental pollutants (Berry et al., 2016; Bambino and Chu, 2017; Lydon et al., 2020), and when coupled to HRMAS NMR metabolic profiling have been effectively used to elucidate integrated pathways of toxicity for these (Roy et al., 2017; Zuberi et al., 2019; Gebreab et al., 2020). In addition to characterizing pathways of toxicity, the suite of metabolites altered by these toxins, furthermore, enables potential identification of biomarkers of exposure and effect, and therefore, has direct value to environmental monitoring and risk assessment efforts.

In the present study, we utilized HRMAS NMR-based metabolic profiling of intact zebrafish embryos to identify metabolic perturbations associated with exposure to PbTx-2. Metabolomics analyses were, furthermore, coupled to an assessment of acute toxicity in embryonic stages of both zebrafish and mahi-mahi (*Coryphaena hippurus*), the latter being an ecologically (i.e., marine) and geographically representative (i.e., endemic to the Gulf of Mexico) species, in order to relate toxicometabolomics to potential impacts on relevant ecological receptors. While toxicity in relation to teleost fish models, in general, has clear relevance to understanding ecotoxicology of PbTx, effects on early life stages of fish represent especially pertinent receptors as toxicity in relation these stages can, in turn, have direct effects on ecosystems including, in particular, population recruitment. Studies were, moreover, conducted in the context of *environmentally relevant concentrations* of PbTx, and thus, may be directly translatable to such ecotoxicological impacts. This approach, thereby, enabled a system-level characterization of the toxicological pathways, and identification of potential biomarkers, of PbTx-2 in environmentally relevant systems. And based on the data obtained, an integrated model of this toxicity, in these system, with consequently direct relevance to ecotoxicology, risk assessment, and identification of biomarkers for monitoring is proposed.

2. Materials and method

2.1. Fish rearing and breeding/spawning

For toxicity testing, zebrafish (*Danio rerio*) embryos (PSA line) were obtained from the University of Miami Rosenstiel School of Marine and Atmospheric Science (UM RSMAS). Rearing and breeding of zebrafish followed previously described procedures (Weiss-Errico et al., 2017; Gebreab et al., 2020). Collected eggs were washed with system water, and transferred to Petri dishes (~120 per "stock" plate) containing approximately 30 mL of E3 medium (Brand et al., 2002). Prior to 72 hour post-fertilization (hpf) exposure, embryos were kept in an incubator (14 h light: 10 h dark, 28 °C), and examined daily to remove any dead or moribund embryos. To facilitate transfer (to test plates), unhatched embryos were typically transferred to wells of test plates prior (~48 hpf) to the 72-hpf exposure. Rearing and breeding was conducted based on protocols approved by University of Miami's Institutional Animal Care and Use Committee (UM IACUC, 20-006 LF), and performed by trained personnel.

For NMR metabolomic studies, zebrafish (OBI/WIK line) embryos were obtained from Helmholtz Centre for Environmental Research (UFZ; Leipzig, Germany). Rearing of adult zebrafish occurred in recirculating aquarium systems, and under previously described procedures (van Amerongen et al., 2014). Breeding included the placement of three adult males and four females in breeding tanks containing mesh egg traps (Ehret GmbH, Emmendingen, Germany) the night prior to collection. Eggs obtained the following morning were observed for any unfertilized/dead embryos and removed prior to adding ~120 embryos to each petri dish containing 40 mL of fresh embryo medium (ISO, 2008) and placed in an incubator with a light cycle of 14 h light: 10 h dark at 28 °C. Each day, dead or disfigured embryos were removed prior to addition of fresh embryo medium. All experimental procedures were performed in agreement with German animal protection standards and approved by the Government of Saxony, Landesdirektion Leipzig, Germany (Aktenzeichen 75-9185.64).

Embryos of mahi-mahi (*Coryphaena hippurus*) were obtained from wild-caught, mating pairs spawned in the UM RSMAS Experimental Hatchery (UMEH). The wild-caught mahi-mahi broodstock were collected from water offshore of Miami, Florida and were transported, acclimated, and spawned according to protocols detailed by Stieglitz et al. (2017). Line-caught fish were transported, as described (Stieglitz et al., 2017), at 26-28 °C until being transferred to quarantine tanks, and subsequently maturation tanks where broodstocks of mahi-mahi were maintained in two 15,000-L fiberglass tanks outfitted with seawater inflows (25–28 °C), and fed daily with a mixture of chopped squid, mackerel, and sardines (Nelson et al., 2016; Kloeblen et al., 2018; Stieglitz et al., 2017). Broodstocks were spawned after 11 days post-capture, and fertilized eggs (i.e., embryos) produced from these spawning events were collected 4–6 h post-spawning, rinsed in UV-sterilized seawater, and transported in a cooler (~30 min transit time) to FIU laboratories for exposure and toxicity testing. All breeding of mahi-mahi was conducted under protocols approved by the UM IACUC (18-052 LF).

2.2. Toxicity of PbTx-2 in zebrafish and mahi-mahi embryos

To evaluate acute toxicity, in general, and additionally establish exposure concentrations for HRMAS-NMR experiments, embryotoxicity (i.e., lethality) was assessed for zebrafish embryos (PSA line) exposed over a concentration range of PbTx-2 (Cayman Chemical, Ann Arbor, MI U.S.A.) at 72 hpf as per previously established and validated protocols (Berry et al., 2007; Weiss-Errico et al., 2017; Gebreab et al., 2020; Lydon et al., 2020). Prior to assays, an exposure concentration range (2, 5, 7.5, 10, 15, 20 and 25 nM PbTx-2) was established in preliminary studies. Subsequently, exposures were conducted in triplicate ($N = 3$) in polypropylene 24-well plates (Evergreen Scientific, Los Angeles, CA) with each well containing 5 embryos ($n = 5$) in 1-mL of E3 medium. An exposure time of 24 h at 72 hpf was selected to allow for the development of vital organs and the nervous system (de Esch et al., 2012), but minimize any chronic effects associated with exposure including general moribundity of embryos. Embryo lethality was determined based on the cessation of movement and absence/presence of heartbeat using a dissecting light microscope.

Embryotoxicity of PbTx-2 toward mahi-mahi embryos (48 hpf), and specifically lethality, was evaluated based on methods adapted, with several modifications, from zebrafish toxicity assays. Mahi-mahi embryos (≤12 hpf) were distributed into 24-well plates with one embryo per well in a total volume of 1 mL of bio-filtered seawater (i.e., 10-μm filtered hatchery system water) into which PbTx-2 was diluted (at 24 hpf). Following preliminary exposure trials, an effective exposure concentration range of 11–67 nM (i.e., 10, 20, 30, 40, 50, and 60 μg/L) PbTx-2 was established for toxicity assays. Each test plate included 6 control wells per plate, and 3 treatments (6 wells each, $n = 6$) with each treatment tested in duplicate (i.e., 2 plates). Assay plates were kept in an incubator on a 16:8 day/night cycle at 25 °C, and observed up to 48 h. Mortality (based on absence of heartbeat, and cessation of movement) was recorded at 48-h using a light microscope. Embryonic development was additionally observed to identify any developmental abnormalities which were photographically documented.

Median lethal concentrations (LC50) were calculated for both species using Probit analysis in SPSS (version 26.0; IBM Corporation, Armonk, NY, USA), and statistically compared based on overlap of calculated 95% confidence intervals. All toxicity assays were conducted at FIU, under protocols approved by the FIU Animal Care and Use Committee (IACUC-19-085 and IACUC-19-104 for mahi-mahi and zebrafish embryos, respectively).

2.3. Exposure of zebrafish embryos for HRMAS-NMR

Exposures for HRMAS-NMR analysis were performed, as previously described (Zuberi et al., 2019), using 72-hpf zebrafish embryos exposed

to 5.5 nM PbTx-2. Embryos (~120 per dish) were specifically exposed to PbTx-2, alongside negative controls (5 μL of solvent, i.e., MeOH, only), in 25 mL of ISO medium in 100-mm polystyrene Petri dishes. After 96 hpf, zebrafish were checked for mortality (and any dead embryos removed), washed 3-times with MilliQ water to remove any residual PbTx-2, and 100 embryos were transferred to a 4-mm zirconium oxide rotor (Bruker BioSpin AG, Switzerland) in which 10 μL of deuterated phosphate buffer (100 mM, pH 7.0) containing 0.1% (*w*/*v*) 3-trimetylsilyl-2,2,3,3-tetradeuteropropionic acid (TSP) was added as a chemical shift reference. All exposures were done in triplicate ($N = 3$).

2.4. HRMAS NMR analysis

Metabolic profiling by HRMAS NMR was performed as adapted from previous studies (Berry et al., 2016; Roy et al., 2017; Zuberi et al., 2019; Gebreab et al., 2020). All NMR experiments were done on a Bruker DMX 600-MHz NMR magnet with a proton resonance frequency of 600 MHz, which was equipped with a 4-mm HRMAS dual $^{1}H/^{13}C$ inverse probe with a magic angle gradient and spinning rate of 6 kHz. Measurements were carried out at a temperature of 277 K using a Bruker BVT3000 control unit. Acquisition and processing of data were done with Bruker TOPSPIN software (Bruker Biospin GmbH, Germany). The ^{1}H HR-MAS NMR spectra were recorded using a standard Bruker pulse sequence "zgpr" (from Bruker's pulse program library) with water presaturation. Each 1D spectrum was acquired applying a spectral width of 12 kHz, time domain (TD) data points 4 k, number of averages 128 with an acquisition time of 170 ms, and a relaxation delay of 2 s. All spectra were processed by an exponential window function corresponding to a line broadening of 1 Hz, and zero-filled, prior to Fourier transformation, using TOPSPIN 3.1 (Bruker Biospin GmbH, Germany). Total analysis time (including sample preparation, optimization of NMR parameters, and data acquisition) of ^{1}H-HRMAS NMR spectroscopy for each sample was approximately 20 min. Sample spinning was 4 min 42 s, and integrity of embryos was not observably affected.

2.5. HRMAS NMR data analysis

Spectra were referenced, baseline- and phase-corrected, and analyzed by using TOPSPIN 3.1 (Bruker Biospin GmbH, Germany). Quantification of metabolites was performed by Chenomx NMR Suite 8.2 (Chenomx Inc., Edmonton, Alberta, Canada). This enabled qualitative and quantitative analysis of NMR spectra by fitting spectral signatures from the Human Metabolome Database (HMDB) to each spectrum. The 600-MHz library from Chenomx was utilized which uses the concentration of a known reference signal (in our case TSP) to determine the concentration of individual compounds. Profiling of the HRMAS NMR spectrum from embryos was accomplished using the *Profiler* module: essentially, a Lorentzian peak shape model of each metabolite is generated from the HMBD information, and superimposed upon the actual spectrum. The area of the peaks from each metabolite is directly related to its abundance. The linear combination of all metabolites gave rise to the total spectral fit, which can be evaluated with a summation line (see Supplementary Fig. S1). The concentrations of metabolites were subsequently calculated based on a ratio relative to tCr (as previously described; Zuberi et al., 2019). Statistical analysis of NMR quantification was done using OriginPro v. 8 (Northampton, USA). Differences in individual metabolites were evaluated using one-way analysis of variance (ANOVA) with a Tukey post-hoc correction for multiple comparisons. A p-value < 0.05 was considered significant. To check the false discovery rate, the p-values were corrected for multiple testing, and q-values were obtained using the Benjamini-Hochberg method (Benjamini and Hochberg, 1995). Levene's test was performed for homogeneity of variance analysis, which indicated that the population variations were not significantly different.

For multivariate analysis, SIMCA software package (Version 14.0, Umetrics, Umeå, Sweden) was used. Bucket tables were generated from the one-dimensional spectra of control and PbTx-2 treated embryos using MestReNova v.12.0.4 (Mestrelab research S.L., Spain). The spectral region between 4.20 and 6.00 ppm was excluded to remove the larger water signal. One-dimensional spectra were normalized to the total intensity and binned into buckets of 0.04 ppm. To compensate for the differences in the overall metabolite concentration between individual samples, the data were mean-centered and scaled using the Pareto method in the SIMCA software package. Both unsupervised principal component analysis (PCA) and supervised partial least-squares discriminant analysis (PLS-DA) were performed on the data using the SIMCA software. The model validation and significance were determined from the R2 value (that indicate how well the model fits the data), and Q2 value (that is a measure of how well the model predicts new data).

2.6. Ex vivo quantitation of glutathione in zebrafish embryos

Reduced glutathione (GSH) was measured ex vivo in extracts of PbTx-exposed and control embryos. Extracts of both treated (5.5 nM PbTx-2) and control zebrafish embryos (96 hpf) were prepared in 5% 5-sulfosalicylic acid, and after centrifugation at 5000 rpm for 5 min, the supernatant used for GSH quantification using an assay kit (Sigma-Aldrich, St. Louis, MO, U.S.A.), according to manufacturers' instruction. Briefly, extracts (10 μL) of control and PbTx-treated embryos were distributed to the 96-well plates and mixed with 150 μL of a working solution which consists of reaction buffer, diluted GSH reductase (enzyme) and 5,5′-dithiobis-2-nitrobenzoic acid (DTNB). After mixing and incubating for 5 min at room temperature, 50 μL of NADPH solution (160 μg/mL) was added to each well, and incubated again for 20 min. Reduced GSH causes a continuous reduction of DTNB to 5-thio2-nitrobenzoic acid (TNB), and the oxidized glutathione (GSSG) formed is recycled by glutathione reductase and NADPH. The yellow product (TNB) was measured spectrophotometrically at 412 nm using a multiplate fluorimeter (Tecan Infinite 200 Pro, Männerdorf, Switzerland).

2.7. Visualization of reactive oxygen species (ROS) in zebrafish embryos

Reactive oxygen species (ROS) generation in the control and PbTx-treated (5.5 nM) zebrafish embryo was visualized in intact zebrafish embryos using the probe chloromethyl-2′,7′-dihydrodichlorofluorescein diacetate (CM-H2DCFA) (Invitrogen™ LSC6827), as a nonfluorescent cell-permeative compound. Intracellular esterases subsequently cleave the acetate groups such that the nonfluorescent dye 2′,7′-dichlorofluorescein (DCF) is retained intracellularly, and in turn, is oxidized by intracellular ROS, and thus becomes fluorescent. At 96 hpf, CM-H2DCFA (1 mM solution in 4% DMSO) was added to control and PbTx-treated (5.5 nM for 24 h) zebrafish embryos in embryo medium (ISO, 2008) to a final concentration of 10 μM, and incubated for another 60 min. Subsequently, embryos were washed 3 times with embryo medium to remove excess CM-H2DCFA in the medium. Embryos were then placed on a borosilicate glass coverslip slide in a solution containing buffer with ethyl 3-aminobenzoate methanesulfonate (1 mg/mL). After a three-minute delay to ensure a steady-state level of anaesthesia, images were captured using an inverted laser-scanning confocal microscope (Leica DMi8/TL LED, Leica Microsystems CMS GmbH) with an excitation wavelength of 485 nm, and emission wavelength of 530 nm. Images were acquired using a Leica HC PL Apo CS2 (5×/0.15 Dry) objective, and Leica Application Suite X (LAS X) software package version 3.1.5.

3. Results and discussion

3.1. Toxicity of PbTx-2 in zebrafish and mahi-mahi embryos

Acute toxicity of PbTx-2 was evaluated in embryonic stages of laboratory raised and bred zebrafish, and wild-caught, and hatchery-spawned, mahi-mahi. Zebrafish including, in particular, early life stages (i.e., embryos, larvae) are a well-established vertebrate toxicological

model, and accordingly, assays for toxicity based on this species (such as those employed herein) have been widely developed, and applied to assess a range of environmental toxicants (Berry et al., 2007; Bambino and Chu, 2017; Weiss-Errico et al., 2017; Gebreab et al., 2020; Lydon et al., 2020). That said, while the zebrafish represents a useful laboratory model, neither the species itself, nor the established laboratory lines of the species, are especially representative of environmentally relevant (i.e., marine) fish as ecological receptors for brevetoxins. The present study, therefore, leveraged the unique availability of mahi-mahi embryos from eggs, spawned within a hatchery, from wild-caught mating pairs to develop and apply toxicity assays (based on those previously developed for zebrafish) to evaluate embryotoxicity of PbTx-2 in this ecologically and commercially relevant species.

Although embryo and larval stages of mahi-mahi have been very recently employed for toxicological assessment of a limited number of environmental pollutants including, in particular, fractions from crude oil associated with oil spills (e.g., Edmunds et al., 2015; Esbaugh et al., 2016; Stieglitz et al., 2016; Nelson et al., 2016; Perrichon et al., 2018; Heuer et al., 2019; Kirby et al., 2019), the present study is the first to utilize this system to assess a relevant marine biotoxin, and specifically PbTx-2 which, in fact, co-occurs with the species within geographically relevant waters (e.g., Gulf of Mexico, southeast Florida). Notably, measured concentrations of Type B brevetoxins, including PbTx-2, in these regional marine waters have been found to typically range from low parts-per-billion (ppb) to parts-per-million (ppm), i.e., nM to μM (Buck and Pierce, 1989; Pierce et al., 2003; Pierce et al., 2005) which is consistent with exposure concentrations evaluated in the current toxicity studies. Furthermore, previous studies have identified PbTx in association with toxicity of sea surface microlayers (SSML) of regionally relevant waters (Rumbold and Snedaker, 1999); and the SSML is, in turn, a key habitat for early life stages (i.e., eggs, embryos and larvae) of marine fish species including mahi-mahi (Wurl and Obbard, 2004). As such, the laboratory toxicity described here, with respect to mahi-mahi, align with environmentally relevant exposure concentrations in geographically and ecologically relevant marine waters.

As physiology and development – and, thus, potential toxicological endpoints – differ considerably between early life stages of the two species, embryo lethality was assessed as a generalized measure of acute toxicity. Among the developmental differences between the two species, mahi-mahi develop more rapidly compared to the zebrafish: while zebrafish typically hatch from chorion as *eleutheroembryos* at approximately 2–3 days post-fertilization (dpf), and subsequently reach larval stages by approximately 7 dpf, embryo development and transition to larval stages in the mahi-mahi approximately occurs within 2 dpf (Perrichon et al., 2019). Median lethal concentration (i.e., LC_{50}) values were accordingly determined in these studies at 48 and 96 hpf, respectively, for mahi-mahi and zebrafish which represent effectively equivalent developmental (i.e., eleutheroembryo) stages for the two species. It was shown (Fig. 1) that PbTx-2 was lethal to embryos of both species at nanomolar concentrations with corresponding LC_{50} values for zebrafish and mahi-mahi, respectively, determined to be 11 nM (95% C.I. = 9.5–13 nM, 96 hpf) and 25 nM (95% C.I. = 19–32 nM, 48 hpf). No mortalities were observed for untreated controls for either species (or corresponding assay format). These results are generally consistent with previous studies that have, likewise, identified a range of relevant toxic effects including mortality, and behavioral and physiological abnormalities (e.g., tachycardia, aberrant swimming behavior of eleutheroembryos) indicative of neurotoxicity, in zebrafish embryos and larvae over the same (i.e., nanomolar) range of exposure concentrations of PbTx-2 (Lydon et al., 2020), as well as toxicity of both Type A and B PbTx to other fish species including both embryonic and adult stages (Shimizu et al., 1986; Rein et al., 1994; Kimm-Brinson and Ramsdell, 2001; Colman and Ramsdell, 2003).

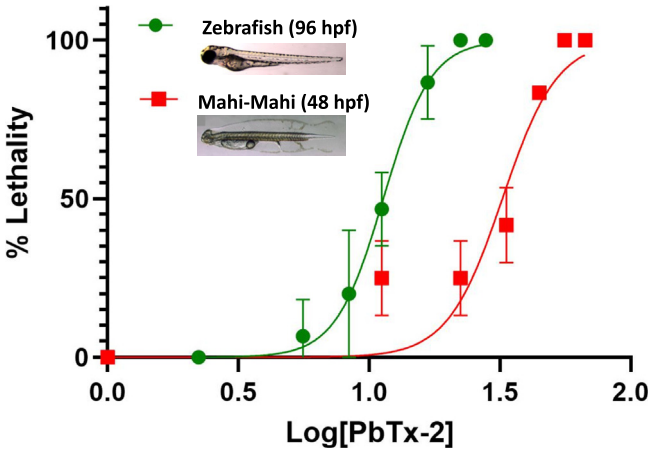

Fig. 1. Dose-dependent acute toxicity of PbTx-2 in early life stages of zebrafish (*Danio rerio*) and mahi-mahi (*Coryphaena hippurus*). Toxicity assessed based on mortality for embryos exposed to PbTx-2 by direct immersion in test solutions, and observed at 96 hpf (24 h exposure) and 48 hpf (48 h exposure), respectively, for *D. rerio* and *C. hippurus*. Log concentration based on nanomolar (nM) concentrations of PbTx-2.

Notably, median lethal concentrations were significantly different ($p < 0.05$) between the two species with higher embryotoxicity observed for zebrafish. This difference may simply reflect a higher sensitivity of the laboratory raised and bred zebrafish, compared to the wild-caught and bred mahi-mahi. All previous studies (Pasparakis et al., 2019; Gebreab et al., forthcomings) that have similarly compared toxicity in the zebrafish and mahi-mahi embryos, however, have generally identified a higher sensitivity of the latter. Studies of Deepwater Horizon oil toxicity, for example, consistently revealed higher sensitivity of mahi-mahi embryos and larvae compared to zebrafish (reviewed by Pasparakis et al., 2019). One very recent study (Gebreab et al., forthcoming), likewise, identified significantly higher acute toxicity (i.e., lower LC_{50}) of several perfluoroalkyl substances for similarly hatchery-spawned mahi-mahi embryos compared to laboratory-reared and bred zebrafish. Alternative explanations may include differential toxicokinetics (i.e., uptake and bioavailability) related, for example, to exposure media (i.e., saltwater versus non-saline medium), or may be related to interspecific differences with respect to targets, mechanisms or pathways of PbTx toxicity. One particularly compelling possibility, in this regard, is the recognized difference in metabolic rates between the two species in relation to the apparent effects of PbTx-2 on energy metabolism, as observed in the present study (discussed below). Indeed, with respect to the latter, metabolic rates of mahi-mahi embryos have been previously found (Pasparakis et al., 2016) to be among the highest reported for teleost fish. That said, possible factors involved in the differential toxicity between the two species remain to be investigated and confirmed in future studies.

Evaluation of toxicity in the zebrafish additionally enabled establishment of suitable exposure concentrations, and other parameters (i.e., developmental stage), for subsequent NMR-based metabolomics studies in this model system. In these subsequent studies, sub-lethal exposure concentrations were selected to avoid any non-specific effects on metabolite profiles due to embryo mortality or morbidity while, at the same time, providing an exposure adequate to elicit a quantifiable metabolic response. Furthermore, an exposure window of 72 hpf was established by these initial toxicity evaluations: at this stage, eleutheroembryos have developed most major organ systems, and in particular, key components (e.g., midbrain-hindbrain boundary, telencephalon, mesencephalon, hypothalamus, primary and secondary motor neurons) of the CNS as the presumptive target of PbTx-2. Accordingly, in these subsequent metabolic profiling studies, 72-hpf embryos were specifically exposed to 5.5 nM PbTx-2 for 24 h. At this exposure concentration, only 6.7% mortality was observed, in toxicity assay, which was not significantly different from untreated controls.

3.2. Oxidative stress in zebrafish embryos exposed to PbTx-2

Oxidative stress as a mechanism for PbTx-2 toxicity was evaluated based on the production ROS in zebrafish embryos. As shown in Fig. 2A, increased levels of ROS were observed in embryos treated with PbTx-2, compared to controls, and specifically in the brain region including telencephalon, mesencephalon and cerebellum. This observation is consistent with both specific uptake and targeting of PbTx-2 to the brain (and reported ability to readily cross the blood-brain barrier), and consequent Ca^{2+} induced production of ROS by mitochondria associated with GluR excitotoxicity. The increase in ROS may, furthermore, be reflected by the highly significant ($p < 0.001$) decrease in GSH, a well-recognized antioxidant, as measured by ex vivo colorimetric assay of embryos (Fig. 2B).

3.3. Altered metabolic profiles of intact zebrafish embryos exposed to PbTx-2 by HRMAS NMR

Well-resolved and quantitative HRMAS NMR spectra of intact zebrafish embryos at 96 hpf (following 24-h exposure time) were obtained (Fig. 3A–B), and when coupled to multivariate analyses including PCA (Fig. 3C–D) and PLS-DA (Fig. S2), revealed significant alteration of numerous metabolites for PbTx-2 treated embryos, compared to untreated, i.e., solvent-only, controls (Fig. 3). Subsequent comparison to the HMDB based on ^{1}H NMR chemical shifts, supplemented by prior 2D NMR (e.g., ^{1}H-^{1}H COSY) analyses of zebrafish (e.g., Zuberi et al., 2019), in turn, enabled unambiguous identification of these metabolites.

In total, 38 metabolites were resolved by HRMAS NMR, and of these, significant changes (i.e., increase or decrease, $p < 0.05$) in 28 metabolites were identified (Table S1). Of these, ten were found to decrease whereas 19 were significantly increased. Significant increases were observed for several metabolites related to energy metabolism including glucose-1-phosphate (G1P, $p < 0.001$), lactate (Lac, $p < 0.01$), citrate (Cit, $p < 0.001$), malate (Mal, $p < 0.05$) and α-ketoglutarate (αKG, $p < 0.005$), along with total fatty acids (FA, $p < 0.001$) and cholesterol (Chol, $p < 0.001$), and several amino acids including aspartate (Asp, $p < 0.001$), asparagine (Asn, $p < 0.005$), glutamate (Glu, $p < 0.001$), glycine (Gly, $p < 0.001$), tryptophan (Trp, $p < 0.001$), phenylalanine (Phe, $p < 0.001$) and tyrosine (Tyr, $p < 0.001$). Increases were additionally observed for the non-proteinogenic amino acid, taurine (Tau, $p < 0.001$), and glycerophosphorylcholine (GPC, $p < 0.01$). Significant decreases, on the other hand, were observed for choline (Cho, $p < 0.001$), *myo*-inositol (*m*-Ins, $p < 0.001$), *N*-acetylaspartate (NAA, $p < 0.001$), fumarate (Fum, $p < 0.05$) and glucose (Glc, $p < 0.001$), as well as *reduced* forms of both nicotinamide adenine dinucleotide (NADH, $p < 0.001$) and glutathione (GSH, $p < 0.001$), and the amino acids glutamine (Gln, $p < 0.001$) and lysine (Lys, $p < 0.001$). Differential alterations were notably observed among components of the *phosphagen system* including decreased levels of creatine (Cr, $p < 0.001$), but elevated levels of both phosphocreatine (pCr, $p < 0.001$) and creatinine (CRN, $p < 0.001$). Taken together, these altered metabolites generally align with several, relevant cellular targets and metabolic pathways including (1) apparent targeting of neural cells and associated neurochemical pathways, i.e., neurotransmission, and (2) mitochondrial oxidative metabolism including interrelated carbohydrate and energy metabolism, and consequent oxidative stress. A summary of the key metabolites associated with these pathways are presented in Fig. 4. And based on the observed alterations of metabolic profiles, an integrated model of the toxicity of PbTx-2 was thereby developed and proposed (see Fig. 5).

3.4. Integrated model of PbTx-2 toxicity based on metabolic profiling

Toxicological research spanning more than four decades (Baden et al., 2005) has clearly identified modulation of VGSC as a primary target of neuronal "excitotoxicity," and specifically allosteric binding to Site 5 of the α-subunit of neuronal VGSC which, in turn, inhibits inactivation of the channel, resulting in sustained depolarization of neurons (Watkins et al., 2008). The action potential resulting from activated VGSC leads to influx of Ca^{2+} through presynaptic voltage-gated calcium channels (VGCC), and the increase of intracellular Ca^{2+} subsequently facilitates fusion of vesicles, and consequent synaptic release of the excitatory neurotransmitter, glutamate (Glu), from neurons (see Fig. 5).

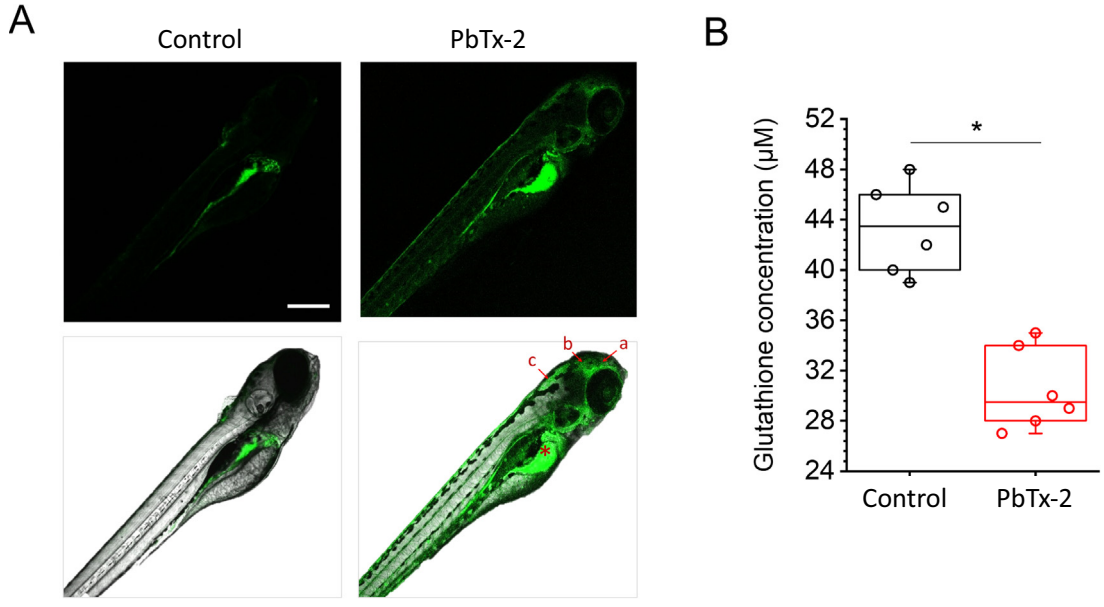

Fig. 2. (A) Localization of reactive oxygen species (ROS) production in zebrafish embryos exposed to PbTx-2 (5.5 nM) as compared to control embryos. Embryos were incubated for 60 min in CM-H2DCFA (10 μM) in rearing medium. Control embryo (left), fluorescence image (top) and overlay with bright field image (bottom). Red arrows highlight the brain region (a, telencephalon; b, mesencephalon; c, cerebellum). Asterisk indicates fluorescent cells in the yolk sac. (B) Glutathione levels in zebrafish embryos exposed to PbTx-2 (5.5 nM for 24 h) as compared to control embryos. Glutathione (GSH) levels in embryo (96 hpf) extracts were analyzed by using GSH assay kit from Sigma-Aldrich. Asterisk indicates significant reduction of GSH ($p < 0.001$, $n = 6$) in PbTx-2 treated embryo is clearly observed. (For interpretation of the references to color in this figure legend, the reader is referred to the web version of this article.)

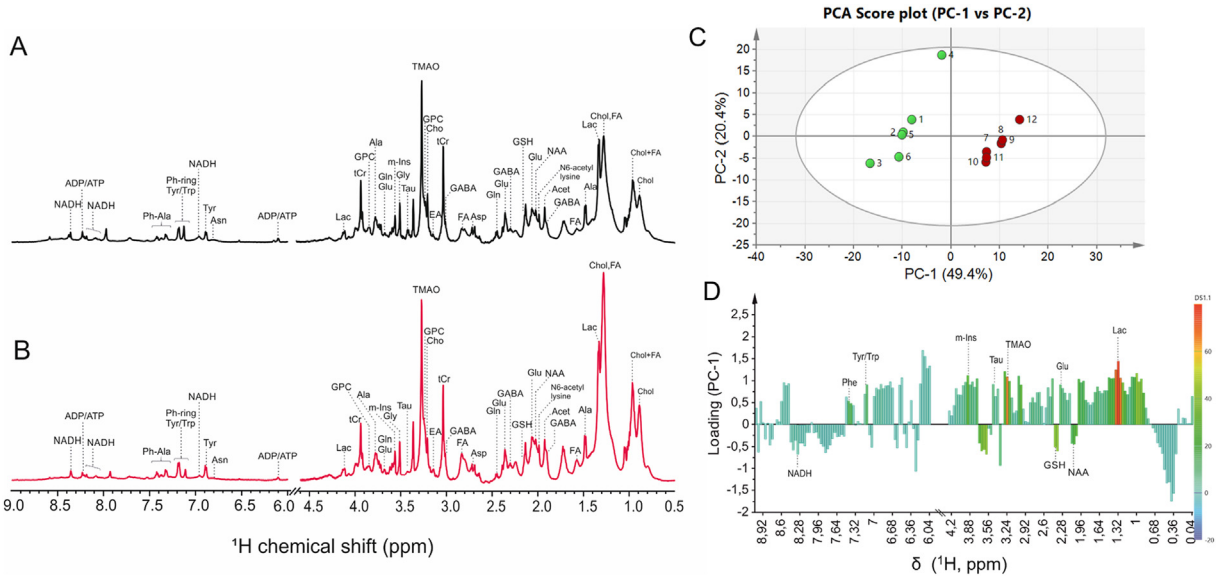

Fig. 3. Representative HRMAS NMR spectra showing metabolic profile of control (A) and PbTx-treated (B) zebrafish embryos, and multivariate analysis (C and D) of the HRMAS NMR data using unbiased principal component analysis (PCA) modelling (R2 = 1, Q2 = 0.999). The scores plot (PC-1 vs PC-2) explains ~70% of total variance of control embryos (1–6) clustering in the negative PC-1 scores, and PbTx-treated (7–12) in the positive PC-1 scores (C). Loading plots of PC-1 (D). Abbreviations: Ala = alanine; Asp = aspartate; Chol = cholesterol; FA = fatty acids; GSH = glutathione; GABA = g-aminobutyric acid; Glc = glucose; Glu = glutamate; Gln = glutamine; GPC = glycerophosphocholine; Gly = glycine; Lac = lactate; m-Ins = *myo*-inositol; Phe = phenylalanine; PC = phosphocholine; Tau = taurine; tCr = total creatine; TMAO = trimethylamine N-oxide; Trp = tryptophan; Tyr = tyrosine.

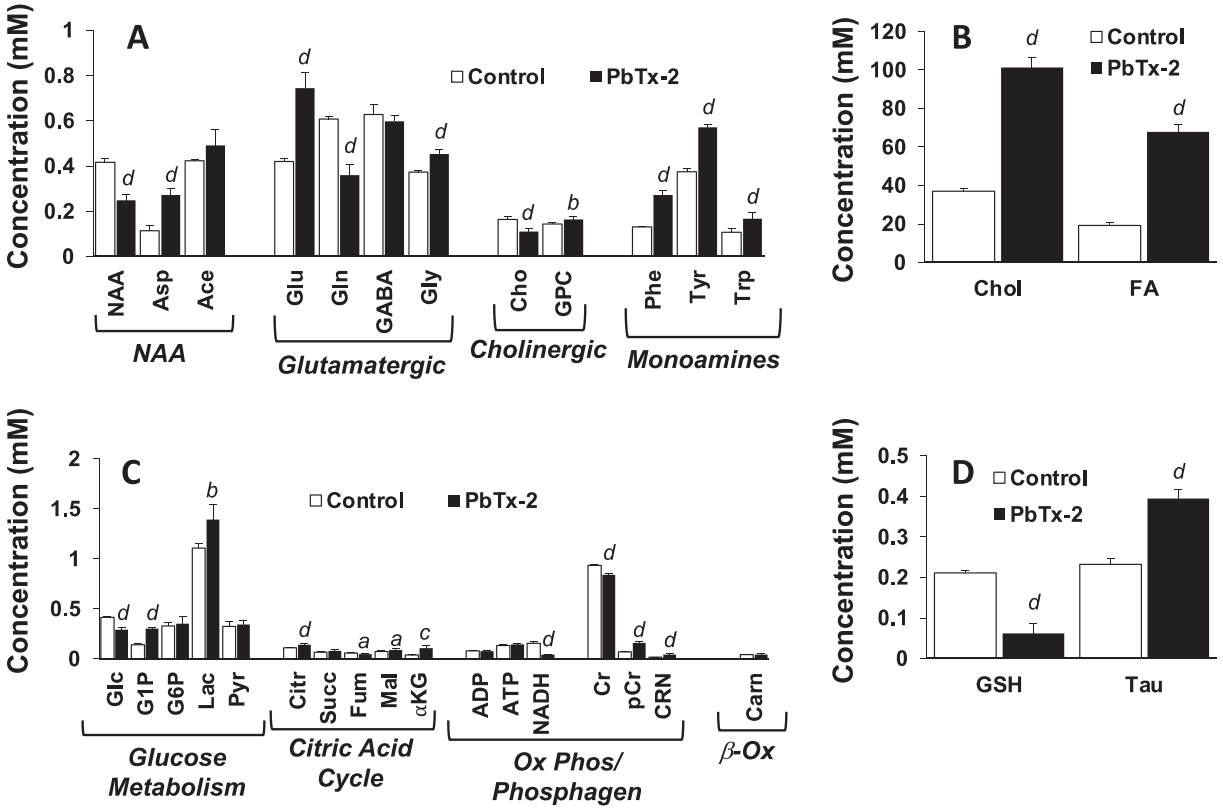

Fig. 4. Summary of key metabolites altered between PbTx-treated and control zebrafish embryos with respect to metabolites associated with (A) neurotoxicity and neurotransmitters; (B) lipid metabolism including total FA and Chol; (C) energy metabolism; and (D) protection against post-synaptic, Ca^{2+}-induced oxidative stress, i.e., Tau and GSH. Proposed pathways associated with metabolites are indicated, including metabolism of *NAA*, *Glutamatergic* and *Cholinergic* pathways, metabolism of *Monamine* neurotransmitters, *Glucose Metabolism*, *Citric Acid Cycle* oxidative phosphorylation ("*Ox Phos*") and *Phosphagen* system, and β-oxidation ("*β-Ox*"). Abbreviations: NAA = *N*-acetylaspartate; Ace = acetate; Asp = aspartate, Glu = glutamate; Gln = glutamine; Gly = glycine; Cho = choline; GPC = glycerophosphorylcholine; Phe = phenylalanine; Tyr = tyrosine; Trp = tryptophan; NADH = nicotinamide adenine dinucleotide; ADP = adenosine diphosphate; ATP = adenosine triphosphate; Glc = glucose; G1P = glucose-1-phosphate; G6P = glucose-6-phosphate; Lac = lactate; Pyr = pyruvate; Cit = citrate; Succ = succinate; Fum = fumarate; Mal = malate; αKG = α-ketoglutarate; Carn = carnitine; Cr = creatine; pCr = phosphocreatine; CRN = creatinine; Chol = cholesterol; FA = fatty acids; Tau = taurine; GSH = glutathione. Metabolite concentrations expressed in mM, normalized to total creatine. Statistical significance: $^{a}p < 0.05$, $^{b}p < 0.01$, $^{c}p < 0.005$ and $^{d}p < 0.001$.

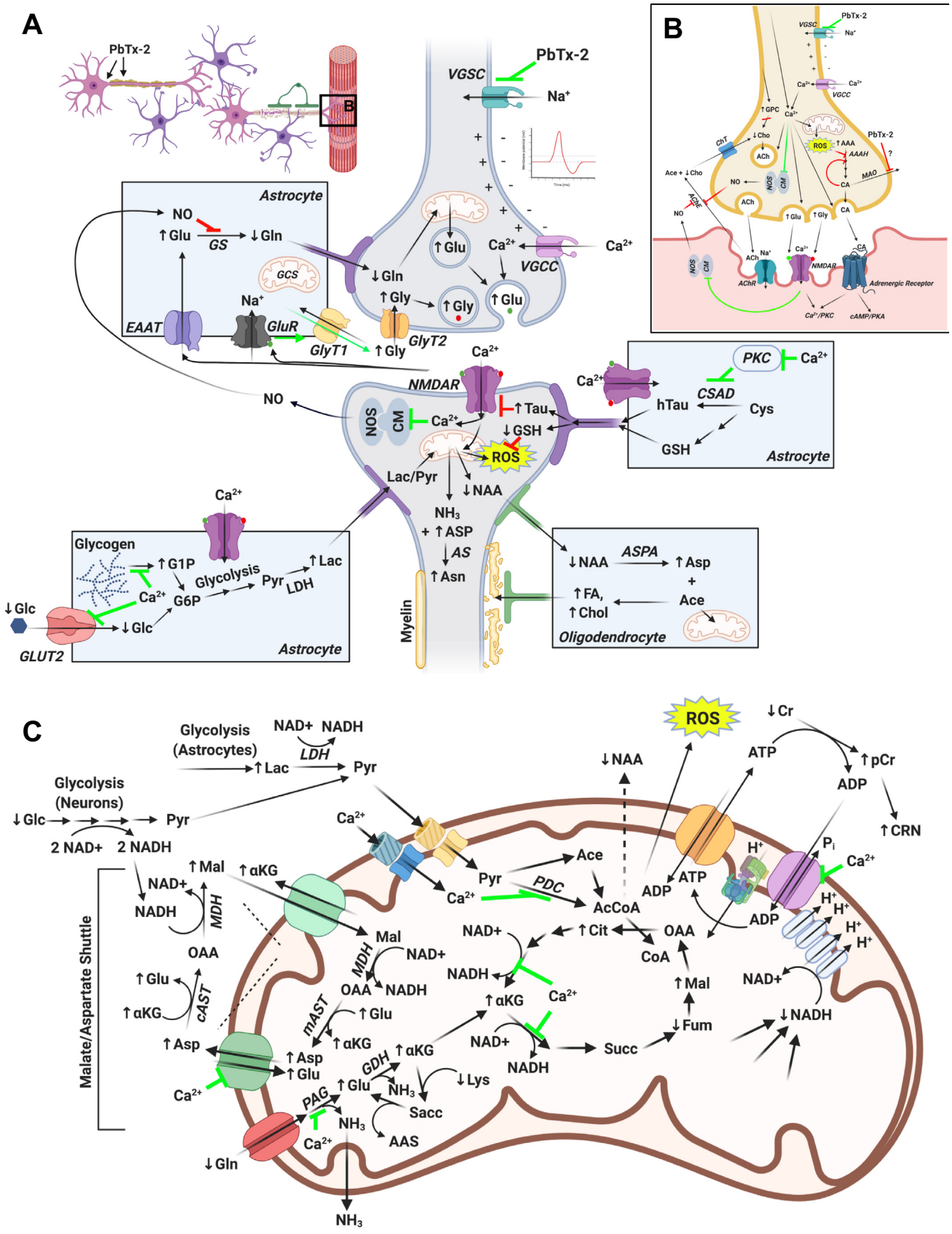
A
PbTx-2
B
VGSC
PbTx-2
Na+
Astrocyte
NO
↑Glu
GS
↓Gln
GCS
↓Gln
↑Glu
Ca2+
Ca2+
VGCC
↑Gly
↑Gly
↑Glu
EAAT
Na+
GluR
GlyT1
↑Gly
GlyT2
Ca2+
NMDAR
NO
NOS
CM
Ca2+
↑Tau
↓GSH
ROS
Lac/Pyr
↓NAA
NH3
+ ↑ASP
AS
↑Asn
Ca2+
PKC
Ca2+
CSAD
hTau
Cys
GSH
Astrocyte
Glycogen
↑G1P
Glycolysis
Pyr
↑Lac
LDH
Ca2+
G6P
↓Glc
↓Glc
GLUT2
Astrocyte
Myelin
↓NAA
ASPA
↑Asp
+
↑FA,
↑Chol
Ace
Oligodendrocyte
B
PbTx-2
VGSC
Na+
Ca2+
VGCC
↑GPC
Ca2+
ChT
↓Cho
ACh
ROS
↑AAA
AAAH
PbTx-2
?
Ace + ↓Cho
NO
NOS
CM
CA
MAO
AChE
NO
ACh
↑Glu
↑Gly
CA
NOS
CM
ACh
Na+
Ca2+
CA
AChR
NMDAR
Adrenergic Receptor
Ca2+/PKC
cAMP/PKA
C
Glycolysis
(Astrocytes)
NAD+ NADH
LDH
↑Lac
Pyr
Glycolysis
(Neurons)
↓Glc
Pyr
2 NAD+ 2 NADH
Ca2+
↑Mal
↑αKG
NAD+
NADH
MDH
OAA
↑Glu
↑αKG
cAST
↑Asp
Ca2+
Malate/Aspartate Shuttle
Mal
MDH
NAD+
OAA
NADH
mAST
↑Glu
↑αKG
↑Asp
↑Glu
GDH
↑αKG
↑Glu
NH3
↓Lys
PAG
NH3
Sacc
Ca2+
AAS
↓Gln
NH3
Ca2+
Pyr
PDC
Ace
AcCoA
NAD+
↑Cit
OAA
NADH
CoA
↑αKG
Ca2+
NAD+
NADH
Succ
↓Fum
↑Mal
ROS
↓NAA
↓Cr
ATP
↑pCr
ADP
↑CRN
ADP
ATP
Pi
Ca2+
H+
ADP
H+
H+
H+
H+
NAD+
↓NADH

Accordingly, the activation of neurons by PbTx-2 has, indeed, been shown to be associated with a concomitant increase in both Ca^{2+} influx (Berman and Murray, 2000; LePage et al., 2003) and Glu release (Berman and Murray, 1999). Glutamate released into synapses subsequently binds and activates glutamate receptors (GluR), and particularly NMDA-type ionotropic GluR (NMDAR), initiating glutamatergic pathways including postsynaptic influx of Ca^{2+} which triggers excitatory post-synaptic potentials (EPSP), alongside initiation of second messenger systems including calmodulin and associated kinases toward long- and short-term neurotransmission (Sheng and Jong Kim, 2002; Dravid et al., 2005). Among the known consequences of the Ca^{2+} influx is altered mitochondrial metabolism including oxidative phosphorylation that, in turn, leads to release of reactive oxygen species (ROS) which can induce neural damage and cell death. In addition to glutamatergic pathways, pre- and postsynaptic influx of Ca^{2+} may similarly modulate other neurotransmitter pathways, as well as various aspects of neural homeostasis. Although alterations in numerous biochemical (i.e., metabolite, protein) and molecular (e.g., gene expression) indicators, consistent with a role of these interrelated pathways, have been reported in relation to the neurotoxicity of PbTx, an holistic *systems-level* understanding of these, and perhaps other, pathways associated with toxicity of PbTx has remained elusive. Systems-level models, however, are effectively enabled by metabolomics approaches, such as the HRMAS NMR metabolite profiling of intact embryos utilized in the present study.

3.4.1. Neuronal targets of PbTx-2 toxicity

Of the metabolites altered by exposure to PbTx-2, several are, indeed, directly aligned with presumptive targeting of neural cells. Significant decreases, for example, were observed for *m*-Ins and NAA (Table S1 and Fig. 4A) that have both been previously established as metabolic biomarkers of neurons and glia (Brand et al., 1993; Schuff et al., 2006; Moffett et al., 2007; Harris et al., 2015). Though *m*-Ins is found in other cell types, it is most abundant and functionally important in glia, and particularly astrocytes, where it contributes to osmotic balance, serves as a precursor to important phospholipids, is a key component of cell membranes, and plays an important role in intracellular signaling (Brand et al., 1993; Harris et al., 2015). On the other hand, NAA is almost exclusively localized to neurons (where it is second only to Glu in abundance), as well as associated oligodendrocytes (Moffett et al., 2007), wherein it similarly serves as an osmolyte and metabolic precursor including supply of acetate for lipids related to myelin synthesis, and for mitochondrial energy production (Moffett et al., 2013). Accordingly, alterations of both *m*-Ins and NAA have, in fact, been employed in NMR, and other magnetic resonance-based techniques, as clinical markers of neural damage (Schuff et al., 2006; Holshouser et al., 2019). Although activation of GluR that accompanies excitotoxicity of PbTx-2 is most frequently associated with neurons (and consequent damage to these cells), it has become increasingly clear that glial cells also express functional GluR (including AMPA, kainite and NMDA-subtypes) such that Glu-mediated excitotoxicity may, in addition, directly damage these neural cell-types (Matute et al., 2007). And the significant decreases in both *m*-Ins and NAA are, therefore, aligned with both neurons and glia as targets of PbTx-2.

Interestingly, decreased NAA coincides with an observed increase in Asp (Fig. 4A) as a building block of the neuronal biosynthesis of this metabolite by *N*-acetyl transferase, and conversely, as a product of its enzymatic hydrolysis/deacetylation by aspartoacylase (ASPA) in oligodendrocytes. Although acetate (similarly a product of enzymatic hydrolysis of NAA, and precursor of NAA biosynthesis) increased as well, the increase was not significant (Table S1); however, it is likely any increase in Ace due to altered biosynthesis or breakdown of NAA might be countered with its diversion (as acetyl CoA) into other metabolic pathways including the tricarboxylic acid (TCA, or "citric acid"; Liu et al., 2018) cycle, and lipid biosynthesis (as discussed below). The reciprocal modulation of NAA and Asp (and presumably Ace) may reflect disruption of neurons, and consequent impairment of enzymatic NAA biosynthesis, or activation of the subsequent hydrolysis of NAA within oligodendrocytes, or perhaps both, as targets of PbTx-2 (Fig. 5). The latter is particularly compelling as CNS myelination is dependent on fatty acid synthesis via NAA-derived acetate, specifically supplied by ASPA, in oligodendrocytes (Francis et al., 2012; Dimas et al., 2019), and GluR-mediated excitotoxicity has, in turn, been linked to myelin damage, specifically at key paranodal regions (Matute et al., 2001; Fu et al., 2009). Supporting this possible mechanism, it has been previously shown that increased synaptic Glu significantly increased expression of ASPA in oligodendrocytes, while inhibition of NMDAR significantly decreased expression, over a relevant (e.g., 8 h) time frame, suggesting a direct link between activation of glutamatergic neurons (as for PbTx-2 excitotoxicity) and rapid glial expression of ASPA toward production of acetate for myelination (Francis et al., 2011). In the present study, levels of lipids (inclusive of both Chol and FA) were, in fact, additionally shown to be significantly increased with exposure to PbTx-2 (Fig. 4B). As such, it is proposed that the observed decreased in NAA with a concurrent increase in Asp and Ace (as hydrolysis products), and increases in lipids (i.e., FA, Chol), may reflect an upregulated compensatory pathway for lipid production in support of myelin repair by oligodendrocytes resulting from PbTx-2 toxicity (Fig. 5).

Consistent with the overarching role of Ca^{2+} in the excitotoxicity, Tau was significantly elevated in PbTx-2 treated embryos (Fig. 4D). Taurine has been shown to reduce influx of Ca^{2+} into neurons through multiple mechanisms including presynaptic VGCC and synaptic neurotransmitter receptors (i.e., NMDAR), as well as from internal (i.e., endoplasmic reticulum) pools, and to increase postsynaptic efflux of Ca^{2+} via Na^{+}/Ca^{2+} exchangers (Chen et al., 2001; Leon et al., 2009; Wu and Prentice, 2010). Increased Tau, therefore, would be consistent with a compensatory mechanism to offset increased Ca^{2+} influx through presynaptic VGCC and/or synaptic GluR in association with PbTx excitotoxicity. With respect to the latter, Dravid et al. (2005) have demonstrated that PbTx-2 leads to augmented Ca^{2+} influx through channels associated with NMDAR, and in turn, it has been shown (Wu and Prentice, 2010; Chan et al., 2013; Chan et al., 2014) that Tau inhibits this influx of Ca^{2+} through these ionotropic receptors. Though it is clear that Tau acts by multiple mechanisms to regulate intracellular Ca^{2+}, the means by which Tau biosynthesis is regulated remains to be clarified. However, it has been suggested (Tang et al., 1997) that Ca^{2+} activates the glial production of hypotaurine, as the immediate precursor of Tau supplied to neurons, and the rate-limiting biosynthetic step from cysteine via protein kinase C-mediated upregulation of cysteine sulfinic acid decarboxylase (CSAD) in astrocytes (Fig. 5).

Fig. 5. (A) Integrated model of pre- and post-synaptic pathways, including role of neuromuscular junctions (B, inset), and (C) pathways associated with mitochondrial energy metabolism in relation to PbTx-2 excitotoxicity, and observed metabolic changes in PbTx-treated zebrafish embryos. Relevant changes (i.e., increase = ↑, decrease = ↓) in metabolites for PbTx-treated zebrafish embryos, relative to negative controls (i.e., solvent vehicle only), are indicated; see Fig. 4 and Table S1 for summary of all metabolites. Abbreviations: *VGSC* = voltage-gated sodium channel, *VGCC* = voltage-gated calcium channel, *NMDA* = NMDA receptor, *CM* = calmodulin, *NOS* = nitric oxide synthetase, *AS* = asparagine synthetase, *EAAT* = excitatory amino acid transporter, *GS* = glutamine synthetase, *GlyT1* = glycine transporter 1, *GlyT2* = glycine transporter 2, *PKC* = protein kinase C, *CSAD* = cysteine sulfinic acid decarboxylase, *GLUT2* = glucose transporter 2, *LDH* = lactate dehydrogenase, *ASPA* = aspartoacylase; hTau = hypotaurine, Cys = cysteine, ROS = reactive oxygen species, NO = nitric oxide; *AAAH* = aromatic amino hydroxylase, *MAO* = monoamine oxidase, *AChR* = acetyl choline receptor, *PKA* = protein kinase A, *PKC* = protein kinase C, *AChE* = acetyl choline esterase, *ChT* = choline transporter; AAA = aromatic amino acids, CA = catecholamine, ACh = acetylcholine, cAMP = cyclic adenosine monophosphate; c*AST* = cytosolic aspartate transaminase, *MDH* = malate dehydrogenase, m*AST* = mitochondrial aspartate transaminase, *PAG* = phosphate-activated glutaminase, *GDH* = glutamate dehydrogenase, *PDC* = pyruvate dehydrogenase complex, *LDH* = lactate dehydrogenase, GCS = glycine cleavage system; AcCoA = acetyl CoA, Sacc = saccharopine, AAS = α-aminoadipate δ-semialdehyde, ROS = reactive oxygen species; for other metabolite abbreviations, see Fig. 4 legend, and Results and discussion text. Green and red lines indicate activation/upregulation and inhibition, respectively. (For interpretation of the references to colour in this figure legend, the reader is referred to the web version of this article.)

Interestingly, a number of Tau-conjugated metabolites of PbTx have been previously identified as part of proposed detoxification mechanisms in both vertebrate and invertebrate, i.e., shellfish, systems (Radwan et al., 2005; Abraham et al., 2012; McNabb et al., 2012); and alternatively, or additionally, elevated levels may thereby reflect upregulation of Tau biosynthesis toward phase II detoxification (i.e., conjugation).

Similarly aligned with downstream effects of excitotoxicity (and, specifically, mitochondrial oxidative metabolism), GSH was significantly decreased in PbTx-exposed embryos (Figs. 2B and 4D). Decreased GSH, as a key antioxidant in neural cells and systems, likely reflects increased oxidative stress, and in particular, ROS that are elevated as a result of increased oxidative phosphorylation by mitochondria following EPSP, and subsequent post-synaptic Ca^{2+} influx associated with excitotoxicity. Indeed, in vivo fluorescence visualization of ROS in 96-hpf zebrafish embryo detected increased production of ROS, and elevated ROS levels were most prominent in the brain region including telencephalon, mesencephalon and cerebellum (Fig. 2A) which further supports CNS as being targeted in embryos at this stage. At the same time, however, it has been shown (Washburn et al., 1996) that PbTx-2 induces glutathione-s-transferase that conjugates GSH to xenobiotics, and subsequently shown, that PbTx-2 undergoes a rapid detoxification via formation of several polar GSH-conjugates (Radwan et al., 2005). This phase II detoxification of PbTx-2 was, furthermore, shown to be similarly accompanied by a depletion of GSH (Walsh et al., 2009). As such, it is proposed that observed reduction in GSH results from the combined direct antioxidant activity, and concurrent depletion by conjugation and detoxification of PbTx-2, by glutathione-based pathways.

3.4.2. Alteration of neurotransmitter pathways

One of the most conspicuous metabolic changes observed for PbTx-exposed embryos is a significant increase in Glu with a concomitant decrease in Gln (Fig. 4A). Glutamate is recognized as the most abundant excitatory neurotransmitter, and moreover, is directly involved in the excitotoxicity of PbTx-2 (Berman and Murray, 1999). And it is, thus, clearly tempting to speculate the elevated levels of Glu reflect this excitotoxicity. As a neurotransmitter, Glu is cycled between neurons and astrocytes (as Gln) via the well-described glutamate/glutamine shuttle: Glu released into synapses is taken-up by excitatory amino acid transporters (EAAT) of astrocytes, wherein it is converted by glutamine synthetase (GS) to Gln which is returned to neurons (Fig. 5) to be effectively recycled by mitochondrial phosphate-activated glutaminases (PAG) to Glu (Fig. 5). While the total concentration of Glu and Gln (i.e., Glx) was not significantly altered (and was, indeed, nearly equal between PbTx-2 treated and control embryos), the Glu/Gln ratio is significantly increased (Table S1) consistent with possible impairment of the recycling of Glu.

It is, thus, proposed that the observed increase in Glu, and concomitant decrease in Gln, may reflect one or more altered metabolic pathways. First, increased Glu/Gln may reflect elevated mitochondrial PAG activity (Fig. 5C) that would increase Glu relative to decreased Gln (as observed). Elevated PAG activity has been shown to accompany glutamate release associated with excitotoxicity (Eid et al., 2007; Fuchsberger et al., 2016), and moreover, it is well established that Ca^{2+} activates PAG as a mechanism for increased glutamate production and release (Kvamme et al., 1983; Albrecht et al., 2010). Aligned with this pathway, a concomitant significant increase in αKG was observed, alongside elevated Glu, in PbTx-exposed embryos: interconversion (Fig. 5C) of Glu and αKG via transamination (of αKG to Glu by aspartate transaminases [AST]) and deamination (of Glu to αKG by glutamate dehydrogenase [GDH]) function, respectively, in the malate/aspartate shuttle to transport NADH from glycolysis into mitochondria, and anaplerotic entry (of αKG) into the citric acid cycle for production of ATP via oxidative phosphorylation (discussed below).

Aligned with sequential deamination of Gln, Glu and αKG - as well as the observed increase in Asp - a significant increase in Asn was, likewise, observed (Table S1). Deamination reactions of both Gln (to Glu) and Glu (to αKG) are associated with production of NH_3, and it is proposed, therefore, that elevated Asn may both reflect the concurrent increase in Asp, and shunting of ammonia to Asn via asparagine synthetase (AS), as an alternative means (to GS which is typically linked to ammonia homeostasis; Zhou et al., 2020) to maintain ammonia levels in the context of the Gln/Glu/αKG conversion pathway. Indeed, deficiencies in AS have been linked to neurodevelopmental defects (Ruzzo et al., 2013), supporting a protective capacity of this enzyme.

Alternatively or additionally, however, it has been shown in previous studies (Kosenko et al., 2003) that Ca^{2+} overloading of postsynaptic neurons can activate nitric oxide synthase (NOS) by way of a calmodulin-dependent pathway, and that resulting nitric oxide (NO) which can readily diffuse into astrocytes may covalently modify (by nitrosylation or nitration) and inhibit activity of GS (Fig. 5), and consequently decrease Gln relative to Glu as observed (Fig. 4A). Consistent with this mechanism, it was previously shown that peripheral blood mononuclear cells from rescued manatees exposed to Florida Red Tide blooms produced significantly higher levels of NO than unexposed animals (Walsh et al., 2007). Furthermore, proteomics studies (Tian et al., 2011) observed that GS was, in fact, down-regulated in medaka embryos exposed to PbTx.

Alongside alterations of Glu metabolism, Gly was notably found to be increased in PbTx-exposed embryos. Glycine is a requisite co-activator of NMDA-type GluR. Synaptic levels of Gly are thought to be maintained by uptake and release by glycine transporters (GlyT) associated with neurons (i.e., GlyT2) and glia (i.e., GlyT1), as well as catabolism of Gly by the *glycine cleavage system* (GCS) which is localized to the mitochondria of astrocytes (Ichinohe et al., 2004; Kikuchi et al., 2008; Zafra et al., 2017). Although regulation of Gly, in relation to glutamatergic pathways, is not well understood, it has been shown that Glu may act through non-NMDA GluR on astrocytes which (through increased Na^+ influx) generates localized membrane depolarization that, in turn leads to efflux of Gly via GlyT1 (Harsing and Matyus, 2013). It is, thus, proposed that increased Gly parallels release of Glu which both acts in concert with Gly at NMDAR, and at the same time, regulates levels of Gly, as part of the integrated effects of PbTx-2 excitotoxicity on glutamatergic pathways (Fig. 5).

In addition to apparent alteration of glutamatergic pathways by PbTx-2, changes in multiple metabolites are, likewise, suggestive of effects on other neurotransmitters. Among these, Cho levels were significantly decreased (Fig. 4A) for PbTx-exposed embryos, relative to controls. Choline has many cellular functions, serving as a component of phospholipids, and as both an osmolyte and methyl donor, in many cell types; in the CNS, however, it is a key component of the neurotransmitter acetylcholine. Synaptic levels of acetylcholine are maintained by the presynaptic biosynthesis (by choline acetyltransferase) and release, and subsequent hydrolytic breakdown by synaptically abundant acetylcholinesterase (AChE) that releases acetate and choline for reuptake and recycling by neurons (Fig. 5B). Acetylcholine is, moreover, the key neurotransmitter at neuromuscular junctions, and NMDAR (as the primary GluR associated with PbTx-2 excitotoxicity; Dravid et al., 2005) have been found to be similarly localized to neuromuscular junctions. Activation of NMDAR has, in turn, been shown (Grozdanovic and Gossrau, 1997; Mays et al., 2009; Personius et al., 2016) to serve as a source of Ca^{2+} for subsequent activation of NOS, and consequently, NMDA-generated NO (which can readily diffuse from pre- and post-synaptic neurons; Schuman and Madison, 1994) that has been shown to act as an effective endogenous inhibitor of AChE (Petrov et al., 2013). This coupling GluR activation to acetylcholine transmission is consistent, in general, with other evidence that suggests synergistic interactions between glutamatergic and cholinergic pathways (Frahm et al., 2015).

Aligned with a role of cholinergic pathways, it has been previously shown that PbTx enhances synaptosomal release of acetylcholine (Nicholson and Kumi, 1991), and that AChE inhibitors potentiate PbTx-induced muscle contractions, specifically via cholinergic pathways (Asai

et al., 1982; Shimoda et al., 1988; Richards and Bourgeois, 2010). More recently, a metabolomic study of medaka (*Oryzias melastigma*) exposed to PbTx found similarly decreased levels of choline, and related this to effects on cholinergic pathways (Yau et al., 2019), and a study of lemon sharks (*Negaprion brevirostris*), exposed to PbTx-containing algal blooms of *K. brevis*, specifically demonstrated a correlation between PbTx exposure level and reduced cholinesterase activity (Nam et al., 2010). Moreover, it has been previously proposed that cholinergic pathways (and their association with neuromuscular junctions) may underlie pulmonary and respiratory symptomology associated with exposure to aerosolized PbTx (Richards et al., 1990; Abraham et al., 2005). Accordingly, it is proposed in the current study that the decrease in Cho observed in the present study may, likewise, reflect either effects on acetylcholine biosynthesis, and subsequent release, or alternatively, indirect (via NO) reduction of the enzymatic hydrolysis of acetylcholine by AChE which, in turn, may contribute to respiratory and pulmonary distress associated with PbTx. Whereas previous studies (e.g., Nam et al., 2010) similarly point to a role of AChE, the current study identified a concomitant increase in GPC suggestive of a possible role of acetylcholine biosynthesis: GPC derived from phosphatidylcholine has been shown to serve as a source of choline for acetylcholine biosynthesis in neural cells (Blusztajn et al., 1987a, 1987b), and the observed increase, therefore, may be consistent with reduced production of choline (Fig. 5).

Further aligned with alterations of other neurotransmitter pathways, aromatic amino acids (AAA) including Trp, Phe and Tyr, were significantly increased in PbTx-treated embryos (Fig. 4A). As *essential* amino acids (i.e., obtained through diet, and not biosynthesized by animals), the biochemical mass balance and, thus, levels of AAA are solely determined by hydrolytic release from proteins and subsequent catabolism, or alternatively, utilization as biosynthetic precursor. Catabolism of AAA, specifically in support of energy metabolism, has been shown to primarily localize to the liver, and although impairment of catabolism via disruption of hepatocytes (i.e., hepatotoxicity) could, thus, explain elevated levels, there is no previous evidence to suggest targeting of hepatocytes by PbTx. Furthermore, trimethylamine N-oxide (TMAO), as a putative biomarker of hepatotoxicity (identified in similar HRMAS NMR studies of the zebrafish embryo model, e.g., Zuberi et al., 2019 and Gebreab et al., 2020), was notably unaltered by PbTx-2 exposure in the present study (Table S1). Alternatively, AAA are known to be biosynthetic precursors of several monoamine neurotransmitters including dopamine and epinephrine/norepinephrine (from Phe/Tyr), and serotonin (from Trp). The first committed and, moreover, rate-limiting step in the biosynthesis of monoamines is specifically carried-out by AAA hydroxylases in neurons (Dickson and Briggs, 2013; Tidemand et al., 2017). These hydroxylases have been shown to be sensitive to ROS, as well as reactive *nitrogen* species (RNS, e.g., peroxynitrite) derived from NO following requisite reactions with ROS (Radi, 2004), and it has been suggested that oxidative state (including ROS and RNS) may serve as a regulating factor for AAA hydroxylase activity and, thus, monoamine neurotransmitter levels (Blanchard-Fillion et al., 2001; Hussain and Mitra, 2004). It is, therefore, proposed that oxidative stress induced by PbTx-2 subsequently inhibits AAA hydroxylase leading to the increased AAA levels observed (Fig. 5B).

Although such a mechanism is plausible, it is confounded by the previous observations which suggest increased levels of catecholamines in association with PbTx exposure. It was found, for example, that PbTx leads to secretion of catecholamines (specifically accompanying Na^+ and Ca^{2+} influx) by sympathetic nerve endings in association with cardiovascular effects (Rodgers et al., 1984; Johnson et al., 1985; Wada et al., 1992). In very recent metabolomics study - specifically employing LC-MS/MS - of medaka (*Oryzias melastigma*), it was similarly shown that catecholamines (i.e., epinephrine) were, likewise, increased in CNS neurotransmitter profiles (Yau et al., 2019). These neurotransmitters themselves are not resolved by HRMAS NMR (in the present study), so their levels in the current studies is unknown. However, the observed increase of catecholamines (in these previous studies) may be reconciled by a previous observation regarding PbTx in the lemon shark: in this study (Nam et al., 2010) activity of monoamine oxidase (MAO) which degrade, and thereby inactivate, catecholamine (and other monamine neurotransmitters) was negatively correlated (i.e., reduced) with exposure to PbTx in *K. brevis* blooms. Thus, elevated levels (as previously observed) may relate to inhibited removal (via MAO), rather than increased production (Fig. 5B). It is, furthermore, known that catecholamines serve as the key end-product feedback inhibitors of AAA hydroxylases (as the rate-limiting step their biosynthesis), and as such, reduced degradation and, consequently, increased levels of the neurotransmitters may additionally contribute (along with ROS) to a further reduced biosynthesis, and elevated levels of AAA precursors, as observed (Fig. 4A).

3.4.3. Perturbation of energy metabolism

Alongside alterations consistent with neurotoxicity, several features of the metabolic profiles point to perturbation of energy metabolism (Fig. 4C) in association with PbTx-2 exposure. Effects of excitotoxicity on energy metabolism would not be surprising given the inordinately high energy requirements of the CNS, in general, and the specifically high portion of this energy budget (in the form of ATP) dedicated to neuronal firing via voltage-gated ion channels, and subsequent Glu-mediated pathways (Shulman et al., 2004; Vergara et al., 2019). With respect to the intersection between excitotoxicity and energy metabolism, Ca^{2+} has been shown (alongside an established role as a key mediator of the excitotoxic response) to upregulate a number of key steps in mitochondrial energy metabolism including enzymes involved in the TCA cycle (e.g., pyruvate dehydrogenase, isocitrate dehydrogenase, α-ketoglutarate dehydrogenase; Denton, 2009), the malate-aspartate shuttle for transporting glycolysis-derived NADH to mitochondria (glutamate-aspartate transporter; Contreras et al., 2007), and the mitochondrial ATP-Mg/Pi carrier (Harborne et al., 2015). It is, therefore, proposed that increased calcium influx toward mitochondria, in association with neuronal excitation by PbTx-2, is likely to contribute - as a central intermediary - to the observed alterations of energy metabolism (Fig. 5).

Aligned with increased energy demands of excitotoxicity, the concomitant decrease in Glc, and increase in G1P, are clearly indicative of elevated catabolism of the carbohydrates to meet these demands. Whereas Glc is the primary currency of carbohydrate metabolism, in general, G1P is exclusively associated with metabolism of glycogen including both biosynthesis (i.e., glycogenesis) and degradation (i.e., glycogenolysis). The concurrent alteration of the two metabolites is, therefore, consistent with metabolic direction of both Glc and G1P (derived, as the first step, from glycogenolysis) via glucose-6-phosphate, as a common intermediate, toward glycolysis (Fig. 5). It has been largely established that glycolysis, supplied by either Glc or glycogenolysis (via G1P), predominantly occurs in astrocytes that specifically supply lactate (generated from pyruvate by lactate dehydrogenase) to neurons which, in turn, convert lactate to pyruvate for entry to the TCA cycle (Deitmer et al., 2019). It has, furthermore, been shown (Magistretti and Allaman, 2018) that glycolysis in astrocytes is, in fact, closely linked to excitability (and, thus, excitotoxicity) of neurons, and that both glucose transporters (i.e., GLUT1) and glycogen phosphorylase (as the rate-limiting step of glycogenolysis) in astrocytes are specifically activated by Ca^{2+} (Glaum et al., 1990; Loaiza et al., 2003). Consistent with this, Lac was, in fact, significantly increased in PbTx-exposed embryos (Fig. 4C). Downstream from glycolysis, Ca^{2+} is known to upregulate key components of the malate-aspartate shuttle including, in particular, the glutamate/aspartate antiporter (GLAST; Palmieri et al., 2001; Contreras et al., 2007) which serves to translocate NADH generated by glycolysis into the mitochondria for oxidative phosphorylation (Fig. 5C). And, indeed, all of the key metabolites associated with the malate/aspartate shuttle significantly increased in PbTx-exposed embryos suggesting elevated activity of this pathway (Fig. 4C). At the same time, Ca^{2+} is known to upregulate pyruvate dehydrogenase as the

primary entry point for pyruvate (as acetyl CoA) into the TCA cycle (Denton, 2009). It is, thus, proposed that increased Ca^{2+} influx both serves to activate glycolysis in astrocytes (Fig. 5), and subsequently direct cytosolic products of glycolysis (i.e., Pyr via Lac) into the mitochondria, and the TCA cycle, of neurons (Fig. 5C).

Of the metabolites associated with the TCA cycle, Cit, Mal and αKG were found to be elevated, whereas Fum decreased, in PbTx-treated embryos (Fig. 4C). Highly significant increases for Cit and αKG are notable given that the former is the entry point for acetyl CoA into the TCA cycle, whereas the latter represents the key intermediate for anaplerotic entry of Glu (via glutamate dehydrogenase) into the TCA cycle. Enzymatic steps both specifically preceding and immediately following αKG (i.e., isocitrate dehydrogenase and α-ketoglutarate dehydrogenase, respectively) are, furthermore, known to be upregulated by Ca^{2+} (Contreras et al., 2007; Denton, 2009), and moreover, both enzymes – as well as *citrate synthase* – are key regulatory steps of the TCA cycle. The observed increase in Mal, and decrease in Fum, on the other hand, likely reflect not only increased activity of the TCA cycle, in general, but also a possible "bottleneck" due to limiting availability of pyruvate-derived acetyl CoA to supply this activity. The potential limitation of this primary substrate of the TCA cycle may, in fact, be reflected by the lack of a significant increase (as discussed above) in acetate: a recent study has specifically shown that during times of "hyperactive" metabolism when demand is high, such as during excitotoxicity, acetate can be directly utilized as an alternative supply of acetyl CoA to the citric acid cycle (Liu et al., 2018). Interestingly, this study showed that this alternative pathway may also utilize a "shunt" of Pyr to acetate by oxidative decarboxylation, specifically utilizing ROS, and as such may simultaneously act as a supplementary antioxidant during times of oxidative stress.

The concomitant increases in Glu and αKG is particularly conspicuous as interconversion of the two metabolites is involved in both anaplerotic entry to the TCA cycle, and the malate-aspartate shuttle (Fig. 5). Alongside these key pathways, however, Glu and αKG are additionally known to be alternatively interconverted as part of the catabolism of Lys, specifically by the *saccharopine pathway* (Fig. 5C). A role of this metabolic pathway is suggested by the highly significant decrease in Lys (Table S1) which, alongside observed increases in Glu and αKG, is clearly indicative of the increased catabolism of this *essential* amino acid in PbTx-exposed embryos (Table S1). Although the function of the saccharopine pathway in animals is not well understood, it has been recently shown to be the predominant catabolic pathway (localized within mitochondria) for this amino acid in the brain (Hallen et al., 2013; Crowther et al., 2019), and along with a presumptive role in lysine homeostasis (which can, in turn, contribute to mitochondrial dysfunction), supplies both NADH and *two equivalents* of acetyl CoA (Zhou et al., 2018).

Finally, although elevated energy production, in association with excitotoxicity, would be expected to specifically increase production of ATP, no significant change in ATP was directly observed in metabolic profiles; however, significant alterations (Fig. 4C) of both NADH and the phosphagen (i.e., Cr/pCr) system do, indeed, align with a shift toward elevated ATP production. With respect to the former, NADH was significantly decreased in PbTx-exposed embryos. This decrease likely reflects increased consumption of the reducing equivalents afforded (for electron transfer) by NADH, specifically supplied by either glycolysis in the cytosol (and transported into mitochondria via malate-aspartate shuttle), or the TCA cycle within the mitochondria, for subsequent oxidative phosphorylation (Fig. 5C). Further linking elevated ATP production by oxidative phosphorylation to excitotoxicity, it is known that Ca^{2+} activates ATP-Mg/P_i carrier, and consequently, transport of adenine nucleotides (for ATP production) into mitochondria (Harborne et al., 2017). Although no significant increase in ATP was directly observed, a significant increase in pCr, and concurrent decrease in Cr, was observed for PbTx-exposed embryos. Phosphorylation of Cr (to pCr) as part of the phosphagen system specifically occurs in neural, myocardial and skeletal muscle cells where it participates in the sequestration, and subsequent turnover, of high energy phosphate bonds (in ATP). It is, therefore, proposed that increased phosphorylation of Cr specifically reflects sequestration of the energy associated with excess ATP generated in association with excitotoxicity in neural cells. At the same time, however, a significant increase in creatinine, as the degradative product of creatine (and phosphocreatine), was observed. This suggests, in parallel, elevated consumption of total creatine (Cr + pCr) as part of the subsequent energy expenditure of cells. And these combined observations, therefore, suggest the phosphagen system effectively represents a shunt for excess energy (i.e., ATP) production associated with excitotoxicity of PbTx-2.

4. Conclusions

The present study further demonstrates the considerable potential of HRMAS NMR when coupled, in particular, to toxicological models (such as zebrafish) for systems-level assessments of environmental toxicants. Metabolic profiling of intact, early life stages of zebrafish exposed, in this case, to PbTx-2 (as the most common congener in marine waters) specifically identified alteration of metabolites (see Table S1 and Fig. 4) associated with both targeting of neural cells and pathways including neuronal excitation (i.e., glutamatergic, cholinergic and adrenergic pathways) and homeostatic functions (i.e., oxidative stress, Ca^{2+}, myelination), and corresponding energy metabolism (i.e., glycolysis, TCA cycle, oxidative phosphorylation) and homeostasis (i.e., phosphagen system). The observed metabolic alterations are, therefore, not only consistent with well recognized and characterized neurotoxicity (i.e., "excitotoxicity") of PbTx, but also align with pathways that may provide insight into other, less understood aspects including respiratory and pulmonary effects (e.g., possible role of cholinergic and adrenergic pathways), and associated cellular energetics. Based on these findings, an integrated model (Fig. 5) is proposed. Although much of this model is, in fact, consistent with current understanding of PbTx toxicity, and neurotoxicology more generally, other components warrant further investigation to validate this proposed model.

Metabolomic studies were coupled, in turn, to an assessment of acute toxicity in embryos of zebrafish and mahi-mahi (Fig. 1). These studies, therefore, not only established toxicity of PbTx-2 in early life stages of fish as potentially relevant environmental receptors, in general, but specifically, an ecologically and geographically relevant species (i.e., mahi-mahi) within an environmentally relevant (i.e., nanomolar) concentration range found in representative (e.g., Gulf of Mexico, Southeastern Atlantic coastal) marine waters. Given the co-occurrence of mahi-mahi and *K. brevis*, as the "Red Tide" producer of PbTx, these studies suggest, therefore, that alteration of metabolic pathways observed, in relation to toxicity, may directly translate to "real world" exposures to perennial blooms of this toxigenic species. Indeed, fish kills (along with marine mammal mortalities) are among the most conspicuous sentinels of Red Tides, and, as such, metabolites and pathways identified in the study might provide insight to effective biomarkers for monitoring of exposure and effects with respect to fisheries, marine mammals and other wildlife specifically.

CRediT authorship contribution statement

Mark Annunziato: Conceptualization, Methodology, Formal analysis, Investigation, Writing – original draft, Writing – review & editing. **Muhamed N.H. Eeza:** Methodology, Formal analysis, Investigation. **Narmin Bashirova:** Investigation. **Ariel Lawson:** Conceptualization, Methodology, Formal analysis, Investigation, Writing – review & editing. **Jörg Matysik:** Resources, Project administration. **Daniel Benetti:** Resources, Writing – review & editing. **Martin Grosell:** Resources, Writing – review & editing. **John D. Stieglitz:** Resources, Writing – review & editing. **A. Alia:** Conceptualization, Methodology, Formal analysis, Investigation, Resources, Writing – review & editing,

Supervision, Project administration, Funding acquisition. **John P. Berry:** Methodology, Formal analysis, Investigation, Resources, Writing – original draft, Writing – review & editing, Supervision, Project administration, Funding acquisition.

Declaration of competing interest

The authors declare that they have no known competing financial interests or personal relationships that could have appeared to influence the work reported in this paper.

Acknowledgments

The authors thank Dr. Pat Gibbs (UM RSMAS) and Dr. Stefan Scholz (UFZ) for generously providing zebrafish embryos in the U.S. and Germany, respectively, and Tianyu Bai (University of Leipzig) for assistance with zebrafish toxicity assays conducted in Germany. Muhamed N. H. Eeza acknowledges the support, through a fellowship, from the Deutscher Akademischer Austauschdienst (DAAD). Research-related travel and other support for Annunziato, Lawson and Berry was funded, in part, from a grant from the U.S. Department of Agriculture (USDA; Grant number NIFA-2017-67018-26229).

Appendix A. Supplementary data

Supplementary data to this article can be found online at https://doi.org/10.1016/j.scitotenv.2021.149858.

References

Abraham, W.M., Bourdelais, A.J., Ahmed, A., Serebriakov, I., Baden, D.G., 2005. Effects of inhaled brevetoxins in allergic airways: toxin-allergen interactions and pharmacologic intervention. Environ. Health Perspect. 113, 632–637. https://doi.org/10.1289/ehp.7498.

Abraham, A., Wang, Y., el Said, K.R., Plakas, S.M., 2012. Characterization of brevetoxin metabolism in karenia brevis bloom-exposed clams (Mercenaria sp.) by LC-MS/MS. Toxicon 60, 1030–1040. https://doi.org/10.1016/j.toxicon.2012.06.016.

Albrecht, P., Lewerenz, J., Dittmer, S., Noack, R., Maher, P., Methner, A., 2010. Mechanisms of oxidative glutamate toxicity: the glutamate/cystine antiporter system xc- as a neuroprotective drug target. CNS Neurol. Disord. Drug Targets 9, 373–382. https://doi.org/10.2174/187152710791292567.

van Amerongen, Y.F., Roy, U., Spaink, H.P., de Groot, H.J., Huster, D., Schiller, J., Alia, A., 2014. Zebrafish brain lipid characterization and quantification by (1)H nuclear magnetic resonance spectroscopy and MALDI-TOF mass spectrometry. Zebrafish 11, 240–247. https://doi.org/10.1089/zeb.2013.0955.

Asai, S., Krzanowski, J.J., Anderson, W.H., Martin, D.F., Poison, J.B., Lockey, R.F., Bukantz, S.C., Szentivanyi, A., 1982. Effects of the toxin of red tide, Ptychodiscus brevis, on canine tracheal smooth muscle: a possible new asthma-triggering mechanism. J. Allergy Clin. Immunol. 69, 418–428. https://doi.org/10.1016/0091-6749(82)90116-6.

Baden, D.G., 1989. Brevetoxins: unique polyether dinoflagellate toxins. FASEB J. 3, 1807–1817. https://doi.org/10.1096/fasebj.3.7.2565840.

Baden, D.G., Bourdelais, A.J., Jacocks, H., Michelliza, S., Naar, J., 2005. Natural and derivative brevetoxins: historical background, multiplicity, and effects. Environ. Health Perspect. 113, 621–625. https://doi.org/10.1289/ehp.7499.

Bakke, M.J., Horsberg, T.E., 2007. Effects of algal-produced neurotoxins on metabolic activity in telecephalon, optic tectum and cerebellum of Atlantic Salmon (Salmo salar). Aquat. Toxicol. 85, 96–103.

Bambino, K., Chu, J., 2017. Chapter nine - zebrafish in toxicology and environmental health. In: Sadler, K.C. (Ed.), Current Topics in Developmental Biology. Academic Press, pp. 331–367. https://doi.org/10.1016/bs.ctdb.2016.10.007.

Benjamini, H., Hochberg, Y., 1995. Controlling the false discovery rate: a practical and powerful approach to multiple testing. J. R. Stat. Soc. Ser. B Stat Methodol. 57, 289–300.

Berman, F.W., Murray, T.F., 1999. Brevetoxins cause acute excitotoxicity in primary cultures of rat cerebellar granule neurons. J. Pharmacol. Exp. Ther. 290, 439–444.

Berman, F.W., Murray, T.F., 2000. Brevetoxin-induced autocrine excitotoxicity is associated with manifold routes of Ca2 influx. J. Neurochem. 74, 1443–1451. https://doi.org/10.1046/j.1471-4159.2000.0741443.x.

Berry, J.P., Gantar, M., Gibbs, P.D.L., Schmale, M.C., 2007. The zebrafish (Danio rerio) embryo as a model system for identification and characterization of developmental toxins from marine and freshwater microalgae. Comp. Biochem. Physiol., Part C: Toxicol. Pharmacol. 145, 61–72. https://doi.org/10.1016/j.cbpc.2006.07.011.

Berry, J.P., Roy, U., Jaja-Chimedza, A., Sanchez, K., Matysik, J., Alia, A., 2016. High-resolution magic angle spinning nuclear magnetic resonance of intact zebrafish embryos detects metabolic changes following exposure to teratogenic polymethoxyalkenes from algae. Zebrafish 13, 456–465. https://doi.org/10.1089/zeb.2016.1280.

Blanchard-Fillion, B., Souza, J.M., Friel, T., Jiang, G.C., Vrana, K., Sharov, V., Barrón, L., Schöneich, C., Quijano, C., Alvarez, B., Radi, R., Przedborski, S., Fernando, G.S., Horwitz, J., Ischiropoulos, H., 2001. Nitration and inactivation of tyrosine hydroxylase by peroxynitrite. J. Biol. Chem. 276, 46017–46023. https://doi.org/10.1074/jbc.m105564200.

Blusztajn, J.K., Liscovitch, M., Mauron, C., Richardson, U.I., Wurtman, R.J., 1987a. Phosphatidylcholine as a precursor of choline for acetylcholine synthesis. J. Neural Transm. Suppl. 24, 247–259.

Blusztajn, J.K., Liscovitch, M., Richardson, U.I., 1987b. Synthesis of acetylcholine from choline derived from phosphatidylcholine in a human neuronal cell line. Proc. Natl. Acad. Sci. U. S. A. 84, 5474–5477. https://doi.org/10.1073/pnas.84.15.5474.

Bourdelais, A.J., Jacocks, H.M., Wright, J.L., Bigwarfe, P.M., Baden, D.G., 2005. A new polyether ladder compound produced by the dinoflagellate karenia brevis. J. Nat. Prod. 68, 2–6.

Brand, M., Granato, M., Nüsslein-Volhard, C., 2002. Keeping and raising zebrafish. Zebrafish 7–37.

Brand, A., Richter-Landsberg, C., Leibfritz, D., 1993. Multinuclear NMR studies on the energy metabolism of glial and neuronal cells. Dev. Neurosci. 15, 289–298. https://doi.org/10.1159/000111347.

Buck, J.D., Pierce, R.H., 1989. Bacteriological aspects of Florida red tides: a revisit and newer obervations. Estuar. Coast. Shelf Sci. 29, 317–326. https://doi.org/10.1016/0272-7714(89)90031-0.

Chan, C.Y., Sun, H.S., Shah, S.M., Agovic, M.S., Ho, I., Friedman, E., Banerjee, S.P., el Idrissi, A., L'Amoreaux, W.J., 2013. Direct Interaction of Taurine with the NMDA Glutamate Receptor Subtype via Multiple Mechanisms. Springer New York, New York, NY, pp. 45–52.

Chan, C.Y., Sun, H.S., Shah, S.M., Agovic, M.S., Friedman, E., Banerjee, S.P., 2014. Modes of direct modulation by taurine of the glutamate NMDA receptor in rat cortex. Eur. J. Pharmacol. 728, 167–175. https://doi.org/10.1016/j.ejphar.2014.01.025.

Chen, W.Q., Jin, H., Nguyen, M., Carr, J., Lee, Y.J., Hsu, C.C., Faiman, M.D., Schloss, J.V., Wu, J.Y., 2001. Role of taurine in regulation of intracellular calcium level and neuroprotective function in cultured neurons. J. Neurosci. Res. 66, 612–619. https://doi.org/10.1002/jnr.10027.

Choich, J., Salierno, J.D., Silbergeld, E.K., Kane, A.S., 2004. Altered brain activity in brevetoxin-exposed bluegill, Lepomis macrochirus, visualized using in vivo 14C 2-deoxyglucose labeling. Environ. Res. 94, 192–197.

Colman, J.R., Ramsdell, J.S., 2003. The type B brevetoxin (PbTx-3) adversely affects development, cardiovascular function, and survival in medaka (Oryzias latipes) embryos. Environ. Health Perspect. 111, 1920–1925. https://doi.org/10.1289/ehp.6386.

Contreras, L., Gomez-Puertas, P., Iijima, M., Kobayashi, K., Saheki, T., Satrústegui, J., 2007. Ca2 activation kinetics of the two aspartate-glutamate mitochondrial carriers, aralar and citrin: ROLE IN THE HEART MALATE-ASPARTATE NADH SHUTTLE*. J. Biol. Chem. 282, 7098–7106. https://doi.org/10.1074/jbc.M610491200.

Crowther, L.M., Mathis, D., Poms, M., Plecko, B., 2019. New insights into human lysine degradation pathways with relevance to pyridoxine-dependent epilepsy due to antiquitin deficiency. J. Inherit. Metab. Dis. 42, 620–628. https://doi.org/10.1002/jimd.12076.

Dechraoui, M.-Y., Naar, J., Pauillac, S., Legrand, A.-M., 1999. Ciguatoxins and brevetoxins, neurotoxic polyether compounds active on sodium channels. Toxicon 37, 125–143. https://doi.org/10.1016/S0041-0101(98)00169-X.

Deitmer, J.W., Theparambil, S.M., Ruminot, I., Noor, S.I., Becker, H.M., 2019. Energy dynamics in the brain: contributions of astrocytes to metabolism and pH homeostasis. Front. Neurosci. 13. https://doi.org/10.3389/fnins.2019.01301.

Denton, R.M., 2009. Regulation of mitochondrial dehydrogenases by calcium ions. Biochim. Biophys. Acta Biomembr. 1787, 1309–1316. https://doi.org/10.1016/j.bbabio.2009.01.005.

Dickson, P.W., Briggs, G.D., 2013. Chapter two - tyrosine hydroxylase: regulation by feedback inhibition and phosphorylation. In: Eiden, L.E. (Ed.), Advances in Pharmacology. Academic Press, pp. 13–21. https://doi.org/10.1016/B978-0-12-411512-5.00002-6.

Dimas, P., Montani, L., Pereira, J.A., Moreno, D., Trötzmüller, M., Gerber, J., Semenkovich, C.F., Köfeler, H.C., Suter, U., 2019. CNS myelination and remyelination depend on fatty acid synthesis by oligodendrocytes. elife. https://doi.org/10.7554/elife.44702.

Dorantes-Aranda, J.J., Seger, A., Mardones, J.I., Nichols, P.D., Hallegraeff, G.M., 2015. Progress in understanding algal bloom-mediated fish kills: the role of superoxide radicals, phycotoxins and fatty acids. PLoS One 10, e0133549. https://doi.org/10.1371/journal.pone.0133549.

Dravid, S.M., Baden, D.G., Murray, T.F., 2005. Brevetoxin augments NMDA receptor signaling in murine neocortical neurons. Brain Res. 1031, 30–38. https://doi.org/10.1016/j.brainres.2004.10.018.

Driggers, W.B., Campbell, M.D., Debose, A.J., Hannan, K.M., Hendon, M.D., Martin, T.L., Nichols, C.C., 2016. Environmental conditions and catch rates of predatory fishes associated with a mass mortality on the West Florida shelf. Estuar. Coast. Shelf Sci. 168, 40–49. https://doi.org/10.1016/j.ecss.2015.11.009.

Edmunds, R.C., Gill, J.A., Baldwin, D.H., Linbo, T.L., French, B.L., Brown, T.L., Esbaugh, A.J., Mager, E.M., Stieglitz, J., Hoenig, R., Benetti, D., Grosell, M., Scholz, N.L., Incardona, J.P., 2015. Corresponding morphological and molecular indicators of crude oil toxicity to the developing hearts of mahi mahi. Sci. Rep. 5, 17326. https://doi.org/10.1038/srep17326.

Eid, T., Hammer, J., Rundén-Pran, E., Roberg, B., Thomas, M.J., Osen, K., Davanger, S., Laake, P., Torgner, I.A., Lee, T.-S.W., Kim, J.H., Spencer, D.D., Ottersen, O.P., de Lanerolle, N.C., 2007. Increased expression of phosphate-activated glutaminase in hippocampal neurons in human mesial temporal lobe epilepsy. Acta Neuropathol. 113, 137–152. https://doi.org/10.1007/s00401-006-0158-5.

Esbaugh, A.J., Mager, E.M., Stieglitz, J.D., Hoenig, R., Brown, T.L., French, B.L., Linbo, T.L., Lay, C., Forth, H., Scholz, N.L., Incardona, J.P., Morris, J.M., Benetti, D.D., Grosell, M., 2016. The effects of weathering and chemical dispersion on Deepwater horizon crude oil

toxicity to mahi-mahi (Coryphaena hippurus) early life stages. Sci. Total Environ. 543, 644–651. https://doi.org/10.1016/j.scitotenv.2015.11.068.
de Esch, C., Slieker, R., Wolterbeek, A., Woutersen, R., de Groot, D., 2012. Zebrafish as potential model for developmental neurotoxicity testing: a mini review. Neurotoxicol. Teratol. 34, 545–553. https://doi.org/10.1016/j.ntt.2012.08.006.
Fire, S.E., Flewelling, L.J., Stolen, M., Durden, W.N., de Wit, M., Spellman, A.C., Wang, Z., 2015. Brevetoxin-associated Mass Mortality Event of Bottlenose Dolphins and Manatees Along the East Coast of Florida, USA. https://doi.org/10.3354/meps11225.
Frahm, S., Antolin-Fontes, B., Görlich, A., Zander, J.-F., Ahnert-Hilger, G., Ibañez-Tallon, I., 2015. An essential role of acetylcholine-glutamate synergy at habenular synapses in nicotine dependence. elife. https://doi.org/10.7554/elife.11396.
Francis, J.S., Strande, L., Pu, A., Leone, P., 2011. Endogenous aspartoacylase expression is responsive to glutamatergic activity in vitro and in vivo. Glia 59, 1435–1446. https://doi.org/10.1002/glia.21187.
Francis, J.S., Strande, L., Markov, V., Leone, P., 2012. Aspartoacylase supports oxidative energy metabolism during myelination. J. Cereb. Blood Flow Metab. 32, 1725–1736. https://doi.org/10.1038/jcbfm.2012.66.
Fu, Y., Sun, W., Shi, Y., Shi, R., Cheng, J.-X., 2009. Glutamate excitotoxicity inflicts paranodal myelin splitting and retraction. PLoS One 4, e6705. https://doi.org/10.1371/journal.pone.0006705.
Fuchsberger, T., Martínez-Bellver, S., Giraldo, E., Teruel-Martí, V., Lloret, A., Viña, J., 2016. Aß induces excitotoxicity mediated by APC/C-Cdh1 depletion that can be prevented by glutaminase inhibition promoting neuronal survival. Sci. Rep. 6, 31158. https://doi.org/10.1038/srep31158.
Gebreab, K.Y., Eeza, M.N.H., Bai, T., Zuberi, Z., Matysik, J., O'Shea, K.E., Alia, A., Berry, J.P., 2020. Comparative toxicometabolomics of perfluorooctanoic acid (PFOA) and next-generation perfluoroalkyl substances. Environ. Pollut. 265, 114928. https://doi.org/10.1016/j.envpol.2020.114928.
Glaum, S.R., Holzwarth, J.A., Miller, R.J., 1990. Glutamate receptors activate Ca2 mobilization and Ca2 influx into astrocytes. Proc. Natl. Acad. Sci. U. S. A. 87, 3454–3458. https://doi.org/10.1073/pnas.87.9.3454.
Gogiashvili, M., Nowacki, J., Hergenröder, R., Hengstler, J.G., Lambert, J., Edlund, K., 2019. HR-MAS NMR based quantitative metabolomics in breast cancer. Metabolites 9, 19.
Grozdanovic, Z., Gossrau, R., 1997. Co-localization of nitric oxide synthase I (NOS I) and NMDA receptor subunit 1 (NMDAR-1) at the neuromuscular junction in rat and mouse skeletal muscle. Cell Tissue Res. 291, 57–63. https://doi.org/10.1007/s004410050979.
Hagger, J.A., Jones, M.B., Leonard, D.R.P., Owen, R., Galloway, T.S., 2006. Biomarkers and integrated environmental risk assessment: are there more questions than answers? Integr. Risk Environ. Assess. Manag. 2, 312–329.
Hallen, A., Jamie, J.F., Cooper, A.J.L., 2013. Lysine metabolism in mammalian brain: an update on the importance of recent discoveries. Amino Acids 45, 1249–1272. https://doi.org/10.1007/s00726-013-1590-1.
Harborne, S.P.D., Ruprecht, J.J., Kunji, E.R.S., 2015. Calcium-induced conformational changes in the regulatory domain of the human mitochondrial ATP-Mg/Pi carrier. Biochim. Biophys. Acta Biomembr. 1847, 1245–1253. https://doi.org/10.1016/j.bbabio.2015.07.002.
Harborne, S.P.D., King, M.S., Crichton, P.G., Kunji, E.R.S., 2017. Calcium regulation of the human mitochondrial ATP-Mg/Pi carrier SLC25A24 uses a locking pin mechanism. Sci. Rep. 7, 45383. https://doi.org/10.1038/srep45383.
Harris, J.L., Choi, I.-Y., Brooks, W.M., 2015. Probing astrocyte metabolism in vivo: proton magnetic resonance spectroscopy in the injured and aging brain. Front. Aging Neurosci. 7. https://doi.org/10.3389/fnagi.2015.00202.
Harsing, L.G., Matyus, P., 2013. Mechanisms of glycine release, which build up synaptic and extrasynaptic glycine levels: the role of synaptic and non-synaptic glycine transporters. Brain Res. Bull. 93, 110–119. https://doi.org/10.1016/j.brainresbull.2012.12.002.
Heuer, R.M., Galli, G.L.J., Shiels, H.A., Fieber, L.A., Cox, G.K., Mager, E.M., Stieglitz, J.D., Benetti, D.D., Grosell, M., Crossley Ii, D.A., 2019. Impacts of Deepwater horizon crude oil on Mahi-Mahi (Coryphaena hippurus) heart cell function. Environ. Sci. Technol. 53, 9895–9904. https://doi.org/10.1021/acs.est.9b03798.
Holshouser, B., Pivonka-Jones, J., Nichols, J.G., Oyoyo, U., Tong, K., Ghosh, N., Ashwal, S., 2019. Longitudinal metabolite changes after traumatic brain injury: a prospective pediatric magnetic resonance spectroscopic imaging study. J. Neurotrauma 36, 1352–1360. https://doi.org/10.1089/neu.2018.5919.
Hussain, A.M., Mitra, A.K., 2004. Effect of reactive oxygen species on the metabolism of tryptophan in rat brain: influence of age. Mol. Cell. Biochem. 258, 145–153. https://doi.org/10.1023/B:MCBI.0000012849.16750.00.
Ichinohe, A., Kure, S., Mikawa, S., Ueki, T., Kojima, K., Fujiwara, K., Iinuma, K., Matsubara, Y., Sato, K., 2004. Glycine cleavage system in neurogenic regions. Eur. J. Neurosci. 19, 2365–2370. https://doi.org/10.1111/j.0953-816X.2004.03345.x.
ISO, 2008. International Standards Organization, Water Quality - Determination of the Acute Toxicity of Waste Water to Zebrafish Eggs (Danio rerio). European Standards ISO, 15088.
Johnson, G.L., Spikes, J.J., Ellis, S., 1985. Cardiovascular effects of brevetoxins in dogs. Toxicon 23, 505–515.
Kikuchi, G., Motokawa, Y., Yoshida, T., Hiraga, K., 2008. Glycine cleavage system: reaction mechanism, physiological significance, and hyperglycinemia. Proc. Jpn. Acad. Ser. B Phys. Biol. Sci. 84, 246–263. https://doi.org/10.2183/pjab.84.246.
Kimm-Brinson, K.L., Ramsdell, J.S., 2001. The red tide toxin, brevetoxin, induces embryo toxicity and developmental abnormalities. Environ. Health Perspect. 109, 377–381. https://doi.org/10.1289/ehp.01109377.
Kirby, A.R., Cox, G.K., Nelson, D., Heuer, R.M., Stieglitz, J.D., Benetti, D.D., Grosell, M., Crossley, D.A., 2019. Acute crude oil exposure alters mitochondrial function and ADP affinity in cardiac muscle fibers of young adult Mahi-mahi (Coryphaena hippurus). Comp. Biochem. Physiol., Part C: Toxicol. Pharmacol. 218, 88–95. https://doi.org/10.1016/j.cbpc.2019.01.004.
Kirkpatrick, B., Fleming, L.E., Squicciarini, D., Backer, L., Clark, R., Abraham, W., Benson, J., Cheng, Y.S., Johnson, D., Pierce, R., Zaias, J., Bossart, G.D., Baden, D.G., 2004. Literature review of Florida red tide: implications for human health effects. Harmful Algae 3, 99–115.
Kirkpatrick, B., Fleming, L.E., Backer, L.C., Bean, J.A., Tamer, R., Kirkpatrick, G., Kane, T., Wanner, A., Dalpra, D., Reich, A., Baden, D.G., 2006. Environmental exposures to Florida red tides: effects on emergency room respiratory diagnoses admissions. Harmful Algae 5, 526–533. https://doi.org/10.1016/j.hal.2005.09.004.
Kloeblen, S., Stieglitz, J.D., Suarez, J.A., Grosell, M., Benetti, D.D., 2018. Characterizing egg quality and larval performance from captive mahi-mahi *Coryphaena hippurus* (Linnaeus, 1758) spawns over time. Aquacult. Res. 49, 282–293.
Kosenko, E., Llansola, M., Montoliu, C., Monfort, P., Rodrigo, R., Hernandez-Viadel, M., Erceg, S., Sánchez-Perez, A.M., Felipo, V., 2003. Glutamine synthetase activity and glutamine content in brain: modulation by NMDA receptors and nitric oxide. Neurochem. Int. 43, 493–499. https://doi.org/10.1016/S0197-0186(03)00039-1.
Kvamme, E., Svenneby, G., Torgner, I.A., 1983. Calcium stimulation of glutamine hydrolysis in synaptosomes from rat brain. Neurochem. Res. 8, 25–38. https://doi.org/10.1007/BF00965651.
Landsberg, J.H., 2002. The effects of harmful algal blooms on aquatic organisms. Rev. Fish. Sci. 10, 113–390.
Leon, R., Wu, H., Jin, Y., Wei, J., Buddhala, C., Prentice, H., Wu, J.-Y., 2009. Protective function of taurine in glutamate-induced apoptosis in cultured neurons. J. Neurosci. Res. 87, 1185–1194. https://doi.org/10.1002/jnr.21926.
LePage, K.T., Baden, D.G., Murray, T.F., 2003. Brevetoxin derivatives act as partial agonists at neurotoxin site 5 on the voltage-gated Na channel. Brain Res. 959, 120–127. https://doi.org/10.1016/S0006-8993(02)03737-X.
Liu, X., Cooper, D.E., Cluntun, A.A., Warmoes, M.O., Zhao, S., Reid, M.A., Liu, J., Lund, P.J., Lopez, M., Garcia, B.A., Wellen, K.E., Kirsch, D.G., Locasale, J.W., 2018. Acetate production from glucose and coupling to mitochondrial metabolism in mammals. Cell 175, 502–513. https://doi.org/10.1016/j.cell.2018.08.040.
Loaiza, A., Porras, O.H., Barros, L.F., 2003. Glutamate triggers rapid glucose transport stimulation in astrocytes as evidenced by real-time confocal microscopy. J. Neurosci. 23, 7337–7342. https://doi.org/10.1523/jneurosci.23-19-07337.2003.
Lombet, A., Bidard, J.-N., Lazdunski, M., 1987. Ciguatoxin and brevetoxins share a common receptor site on the neuronal voltage-dependent Na+ channel. FEBS Lett. 219, 355–359. https://doi.org/10.1016/0014-5793(87)80252-1.
Lu, Z., Tomchik, S.M., 2002. Effects of a red-tide toxin on fish hearing. J. Comp. Physiol. A Neuroethol. Sens. Neural Behav. Physiol. 188, 807–813.
Lucas-Torres, C., Wong, A., 2020. Intact NMR spectroscopy: slow high-resolution magic angle spinning chemical shift imaging. Analyst 145, 2520–2524. https://doi.org/10.1039/d0an00118j.
Lydon, C.A., Mathivathanan, L., Sanchez, J., dos Santos, L.A.H., Sauvage, T., Gunasekera, S.P., Paul, V.J., Berry, J.P., 2020. Eudesmacarbonate, a eudesmane-type sesquiterpene from a marine filamentous cyanobacterial mat (Oscillatoriales) in the Florida keys. J. Nat. Prod. 83, 2030–2035. https://doi.org/10.1021/acs.jnatprod.0c00203.
Magistretti, P.J., Allaman, I., 2018. Lactate in the brain: from metabolic end-product to signalling molecule. Nat. Rev. Neurosci. 19, 235–249. https://doi.org/10.1038/nrn.2018.19.
Matute, C., Alberdi, E., Domercq, M., Pérez-Cerdá, F., Pérez-Samartí´n, A., Sánchez-Gómez, M.V., 2001. The link between excitotoxic oligodendroglial death and demyelinating diseases. Trends Neurosci. 24, 224–230. https://doi.org/10.1016/S0166-2236(00)01746-X.
Matute, C., Alberdi, E., Domercq, M., Sánchez-Gómez, M.-V., Pérez-Samartín, A., Rodríguez-Antigüedad, A., Pérez-Cerdá, F., 2007. Excitotoxic damage to white matter. J. Anat. 210, 693–702. https://doi.org/10.1111/j.1469-7580.2007.00733.x.
Mays, T.A., Sanford, J.L., Hanada, T., Chishti, A.H., Rafael-Fortney, J.A., 2009. Glutamate receptors localize postsynaptically at neuromuscular junctions in mice. Muscle Nerve 39, 343–349. https://doi.org/10.1002/mus.21099.
McNabb, P.S., Selwood, A.I., van Ginkel, R., Boundy, M., Holland, P.T., 2012. Determination of brevetoxins in shellfish by LC/MS/MS: single-laboratory validation. J. AOAC Int. 95, 1097–1105. https://doi.org/10.5740/jaoacint.11-272.
Moffett, J.R., Ross, B., Arun, P., Madhavarao, C.N., Namboodiri, A.M.A., 2007. N-acetylaspartate in the CNS: from neurodiagnostics to neurobiology. Prog. Neurobiol. 81, 89–131. https://doi.org/10.1016/j.pneurobio.2006.12.003.
Moffett, J., Arun, P., Ariyannur, P., Namboodiri, A., 2013. N-acetylaspartate reductions in brain injury: impact on post-injury neuroenergetics, lipid synthesis, and protein acetylation. Front. Neuroenerg. 5. https://doi.org/10.3389/fnene.2013.00011.
Nam, D.-H., Adams, D.H., Flewelling, L.J., Basu, N., 2010. Neurochemical alterations in lemon shark (Negaprion brevirostris) brains in association with brevetoxin exposure. Aquat. Toxicol. 99, 351–359. https://doi.org/10.1016/j.aquatox.2010.05.014.
Nelson, D., Heuer, R.M., Cox, G.K., Stieglitz, J.D., Hoenig, R., Mager, E.M., Benetti, D.D., Grosell, M., Crossley, D.A., 2016. Effects of crude oil on in situ cardiac function in young adult mahi–mahi (Coryphaena hippurus). Aquat. Toxicol. 180, 274–281. https://doi.org/10.1016/j.aquatox.2016.10.012.
Nicholson, R.A., Kumi, C.O., 1991. The effects of pesticides, brevetoxin B, and the cardiotonic drug DPI 201 106 on release of acetylcholine from insect central nerve terminals. Pestic. Biochem. Physiol. 40, 86–97. https://doi.org/10.1016/0048-3575(91)90051-M.
Palmieri, L., Pardo, B., Lasorsa, F.M., del Arco, A., Kobayashi, K., Iijima, M., Runswick, M.J., Walker, J.E., Saheki, T., Satrústegui, J., Palmieri, F., 2001. Citrin and aralar1 are Ca(2)-stimulated aspartate/glutamate transporters in mitochondria. EMBO J. 20, 5060–5069. https://doi.org/10.1093/emboj/20.18.5060.
Pasparakis, C., Mager, E.M., Stieglitz, J.D., Benetti, D., Grosell, M., 2016. Effects of Deepwater horizon crude oil exposure, temperature and developmental stage on oxygen

consumption of embryonic and larval mahi-mahi (Coryphaena hippurus). Aquat. Toxicol. 181, 113–123. https://doi.org/10.1016/j.aquatox.2016.10.022.
Pasparakis, C., Esbaugh, A.J., Burggren, W., Grosell, M., 2019. Physiological impacts of Deepwater Horizon oil on fish. Comp. Biochem. Physiol., Part C: Toxicol. Pharmacol. 224, 108558.
Perrichon, P., Mager, E.M., Pasparakis, C., Stieglitz, J.D., Benetti, D.D., Grosell, M., Burggren, W.W., 2018. Combined effects of elevated temperature and Deepwater Horizon oil exposure on the cardiac performance of larval mahi-mahi, Coryphaena hippurus. PLoS One 13, e0203949. https://doi.org/10.1371/journal.pone.0203949.
Perrichon, P., Stieglitz, J.D., Xu, E.G., Magnuson, J.T., Pasparakis, C., Mager, E.M., Wang, Y., Schlenk, D., Benetti, D.D., Roberts, A.P., Grosell, M., Burggren, W.W., 2019. Mahi-mahi (Coryphaena hippurus) life development: morphological, physiological, behavioral and molecular phenotypes. Dev. Dyn. 248, 337–350. https://doi.org/10.1002/dvdy.27.
Personius, K.E., Slusher, B.S., Udin, S.B., 2016. Neuromuscular NMDA receptors modulate developmental synapse elimination. J. Neurosci. 36, 8783–8789. https://doi.org/10.1523/jneurosci.1181-16.2016.
Petrov, K.A., Malomouzh, A.I., Kovyazina, I.V., Krejci, E., Nikitashina, A.D., Proskurina, S.E., Zobov, V.V., Nikolsky, E.E., 2013. Regulation of acetylcholinesterase activity by nitric oxide in rat neuromuscular junction via N-methyl-d-aspartate receptor activation. Eur. J. Neurosci. 37, 181–189. https://doi.org/10.1111/ejn.12029.
Pierce, R.H., Henry, M.S., Blum, P.C., Lyons, J., Cheng, Y.S., Yazzie, D., Zhou, Y., 2003. Brevetoxin concentrations in marine aerosol: human exposure levels during a karenia brevis harmful algal bloom. Bull. Environ. Contam. Toxicol. 70, 161–165. https://doi.org/10.1007/s00128-002-0170-y.
Pierce, R.H., Henry, M.S., Blum, P.C., Hamel, S.L., Kirkpatrick, B., Cheng, Y.S., Zhou, Y., Irvin, C.M., Naar, J., Weidner, A., Fleming, L.E., Backer, L.C., Baden, D.G., 2005. Brevetoxin composition in water and marine aerosol along a Florida beach: assessing potential human exposure to marine biotoxins. Harmful Algae 4, 965–972. https://doi.org/10.1016/j.hal.2004.11.004.
Pierce, R.H., Henry, M.S., Blum, P.C., Osborn, S.E., Cheng, Y.-S., Zhou, Y., Irvin, C.M., Bourdelais, A.J., Naar, J., Baden, D.G., 2010. Compositional changes in neurotoxins and their oxidative derivatives from the dinoflagellate, karenia brevis, in seawater and marine aerosol. J. Plankton Res. 33, 343–348. https://doi.org/10.1093/plankt/fbq115.
Pierre, O., Misery, L., Talagas, M., le Garrec, R., 2018. Immune effects of the neurotoxins ciguatoxins and brevetoxins. Toxicon 149, 6–19. https://doi.org/10.1016/j.toxicon.2018.01.002.
Radi, R., 2004. Nitric oxide, oxidants, and protein tyrosine nitration. Proc. Natl. Acad. Sci. U. S. A. 101, 4003–4008. https://doi.org/10.1073/pnas.0307446101.
Radwan, F.F.Y., Wang, Z., Ramsdell, J.S., 2005. Identification of a rapid detoxification mechanism for brevetoxin in rats. Toxicol. Sci. 85, 839–846. https://doi.org/10.1093/toxsci/kfi138.
Rein, K.S., Lynn, B., Gawley, R.E., Baden, D.G., 1994. Brevetoxin B: chemical modifications, synaptosome binding, toxicity, and an unexpected conformational effect. J. Org. Chem. 59, 2107–2113. https://doi.org/10.1021/jo00087a028.
Richards, I.S., Bourgeois, M., 2010. Red tide toxin produces in vitro depolarization of human airway smooth muscle. Clin. Toxicol. (Phila.) 48, 121–123. https://doi.org/10.3109/15563650903476483.
Richards, I.S., Kulkarni, A.P., Brooks, S.M., Pierce, R., 1990. Florida red-tide toxins (brevetoxins) produce depolarization of airway smooth muscle. Toxicon 28, 1105–1111. https://doi.org/10.1016/0041-0101(90)90149-2.
Rodgers, R.L., Chou, H.-N., Temma, K., Akera, T., Shimizu, Y., 1984. Positive inotropic and toxic effects of brevetoxin-B on rat and Guinea pig heart. Toxicol. Appl. Pharmacol. 76, 296–305. https://doi.org/10.1016/0041-008X(84)90011-5.
Roy, U., Conklin, L., Schiller, J., Matysik, J., Berry, J.P., Alia, A., 2017. Metabolic profiling of zebrafish (Danio rerio) embryos by NMR spectroscopy reveals multifaceted toxicity of ß-methylamino-L-alanine (BMAA). Sci. Rep. 7, 17305. https://doi.org/10.1038/s41598-017-17409-8.
Rumbold, D., Snedaker, S., 1999. Sea-surface microlayer toxicity off the Florida keys. Mar. Environ. Res. 47, 457–472. https://doi.org/10.1016/S0141-1136(98)00131-7.
Ruzzo, E.K., Capo-Chichi, J.-M., Ben-Zeev, B., Chitayat, D., Mao, H., Pappas, A.L., Hitomi, Y., Lu, Y.-F., Yao, X., Hamdan, F.F., Pelak, K., Reznik-Wolf, H., Bar-Joseph, I., Oz-Levi, D., Lev, D., Lerman-Sagie, T., Leshinsky-Silver, E., Anikster, Y., Ben-Asher, E., Olender, T., Colleaux, L., Décarie, J.-C., Blaser, S., Banwell, B., Joshi, R.B., He, X.-P., Patry, L., Silver, R.J., Dobrzeniecka, S., Islam, M.S., Hasnat, A., Samuels, M.E., Aryal, D.K., Rodriguiz, R.M., Jiang, Y., Wetsel, W.C., McNamara, J.O., Rouleau, G.A., Silver, D.L., Lancet, D., Pras, E., Mitchell, G.A., Michaud, J.L., Goldstein, D.B., 2013. Deficiency of asparagine synthetase causes congenital microcephaly and a progressive form of encephalopathy. Neuron 80, 429–441. https://doi.org/10.1016/j.neuron.2013.08.013.
Salierno, J.D., Snyder, N.S., Murphy, A.Z., Poli, M., Hall, S., Baden, D., Kane, A.S., 2006. Harmful algal bloom toxins alter c-fos protein expression in the brain of killifish, Fundulus heteroclitus. Aquat. Toxicol. 78, 350–357.
Schuff, N., Meyerhoff, D.J., Mueller, S., Chao, L., Sacrey, D.T., Laxer, K., Weiner, M.W., Moffett, J.R., Tieman, S.B., Weinberger, D.R., Coyle, J.T., Namboodiri, A.M.A., 2006. N-Acetylaspartate as a Marker of Neuronal Injury in Neurodegenerative Disease. Springer US, Boston, MA, pp. 241–262.
Schuman, E.M., Madison, D.V., 1994. Nitric oxide and synaptic function. Annu. Rev. Neurosci. 17, 153–183. https://doi.org/10.1146/annurev.ne.17.030194.001101.
Sheng, M., Jong Kim, M., 2002. Postsynaptic signaling and plasticity mechanisms. Science 298, 776. https://doi.org/10.1126/science.1075333.
Shimizu, Y., Chou, H.N., Bando, H., van Duyne, G., Clardy, J., 1986. Structure of brevetoxin a (GB-1 toxin), the most potent toxin in the Florida red tide organism Gymnodinium breve (Ptychodiscus brevis). J. Am. Chem. Soc. 108, 514–515. https://doi.org/10.1021/ja00263a031.
Shimoda, T., Krzanowski, J., Nelson, R., Martin, D.F., Polson, J., Duncan, R., Lockey, R., 1988. In vitro red tide toxin effects on human bronchial smooth muscle. J. Allergy Clin. Immunol. 81, 1187–1191. https://doi.org/10.1016/0091-6749(88)90889-5.
Shulman, R.G., Rothman, D.L., Behar, K.L., Hyder, F., 2004. Energetic basis of brain activity: implications for neuroimaging. Trends Neurosci. 27, 489–495. https://doi.org/10.1016/j.tins.2004.06.005.
Stieglitz, J.D., Mager, E.M., Hoenig, R.H., Benetti, D.D., Grosell, M., 2016. Impacts of Deepwater horizon crude oil exposure on adult mahi-mahi (Coryphaena hippurus) swim performance. Environ. Toxicol. Chem. 35, 2613–2622. https://doi.org/10.1002/etc.3436.
Stieglitz, J.D., Hoenig, R.H., Kloeblen, S., Tudela, C.E., Grosell, M., Benetti, D.D., 2017. Capture, transport, prophylaxis, acclimation, and continuous spawning of Mahi-mahi (Coryphaena hippurus) in captivity. Aquaculture 479, 1–6. https://doi.org/10.1016/j.aquaculture.2017.05.006.
Tang, X.W., Hsu, C.C., Schloss, J.V., Faiman, M.D., Wu, E., Yang, C.Y., Wu, J.Y., 1997. Protein phosphorylation and taurine biosynthesis in vivo and in vitro. J. Neurosci. Off. J. Soc. Neurosci. 17, 6947–6951. https://doi.org/10.1523/JNEUROSCI.17-18-06947.1997.
Tian, L., Wang, Minghua, Li, X., Lam, P.K.S., Wang, Mingfu, Wang, D., Chou, H.N., Li, Y., Chan, L.L., 2011. Proteomic modification in gills and brains of medaka fish (oryzias melastigma) after exposure to a sodium channel activator neurotoxin, brevetoxin-1. Aquat. Toxicol. 104, 211–217. https://doi.org/10.1016/j.aquatox.2011.04.019.
Tidemand, K.D., Peters, G.H., Harris, P., Stensgaard, E., Christensen, H.E.M., 2017. Isoform-specific substrate inhibition mechanism of human tryptophan hydroxylase. Biochemistry 56, 6155–6164. https://doi.org/10.1021/acs.biochem.7b00763.
Trainer, V.L., Moreau, E., Guedin, D., Baden, D.G., Catterall, W.A., 1993. Neurotoxin binding and allosteric modulation at receptor sites 2 and 5 on purified and reconstituted rat brain sodium channels. J. Biol. Chem. 268, 17114–17119.
Tuladhar, A., Hondal, R.J., Colon, R., Hernandez, E.L., Rein, K.S., 2019. Effectors of thioredoxin reductase: brevetoxins and manumycin-a. Comp. Biochem. Physiol., Part C: Toxicol. Pharmacol. 217, 76–86. https://doi.org/10.1016/j.cbpc.2018.11.015.
Vergara, R.C., Jaramillo-Riveri, S., Luarte, A., Moënne-Loccoz, C., Fuentes, R., Couve, A., Maldonado, P.E., 2019. The energy homeostasis principle: neuronal energy regulation drives local network dynamics generating behavior. Front. Comput. Neurosci. 13. https://doi.org/10.3389/fncom.2019.00049.
Wada, A., Uezono, Y., Arita, M., Yuhi, T., Kobayashi, H., Yanagihara, N., Izumi, F., 1992. Co-operative modulation of voltage-dependent sodium channels by brevetoxin and classical neurotoxins in cultured bovine adrenal medullary cells. J. Pharmacol. Exp. Ther. 263, 1347–1351.
Walsh, C.J., Stuckey, J.E., Cox, H., Smith, B., Funke, C., Stott, J., Colle, C., Gaspard, J., Manire, C.E., 2007. Production of nitric oxide by peripheral blood mononuclear cells from the Florida manatee, *Trichechus manatus latirostris*. Vet. Immunol. Immunopathol. 118, 199–209.
Walsh, C.J., Leggett, S.R., Henry, M.S., Blum, P.C., Osborn, S., Pierce, R.H., 2009. Cellular metabolism of brevetoxin (PbTx-2) by a monocyte cell line (U-937). Toxicon 53, 135–145. https://doi.org/10.1016/j.toxicon.2008.10.024.
Washburn, B.S., Vines, C.A., Baden, D.G., Hinton, D.E., Walsh, P.J., 1996. Differential effects of brevetoxin and β-naphthoflavone on xenobiotic metabolizing enzymes in striped bass (*Morone saxatilis*). Aquat. Toxicol. 35, 1–10.
Watkins, S.M., Reich, A., Fleming, L.E., Hammond, R., 2008. Neurotoxic shellfish poisoning. Mar. Drugs 6, 431–455.
Weiss-Errico, M.J., Berry, J.P., O'Shea, K.E., 2017. ß-cyclodextrin attenuates perfluorooctanoic acid toxicity in the zebrafish embryo model. Toxics 5, 31.
Wu, J.-Y., Prentice, H., 2010. Role of taurine in the central nervous system. J. Biomed. Sci. 17, S1. https://doi.org/10.1186/1423-0127-17-S1-S1.
Wurl, O., Obbard, J.P., 2004. A review of pollutants in the sea-surface microlayer (SML): a unique habitat for marine organisms. Mar. Pollut. Bull. 48, 1016–1030. https://doi.org/10.1016/j.marpolbul.2004.03.016.
Yau, M.-S., Lei, E.N.-Y., Ng, I.H.-M., Yuen, C.K.-K., Lam, J.C.-W., Lam, M.H.-W., 2019. Changes in the neurotransmitter profile in the central nervous system of marine medaka (Oryzias melastigma) after exposure to brevetoxin PbTx-1 – a multivariate approach to establish exposure biomarkers. Sci. Total Environ. 673, 327–336. https://doi.org/10.1016/j.scitotenv.2019.03.193.
Zafra, F., Ibáñez, I., Bartolomé-Martín, D., Piniella, D., Arribas-Blázquez, M., Giménez, C., 2017. Glycine transporters and its coupling with NMDA receptors. In: Ortega, A., Schousboe, A. (Eds.), Glial Amino Acid Transporters. Springer International Publishing, Cham, pp. 55–83. https://doi.org/10.1007/978-3-319-55769-4_4.
Zhou, J., Wang, X., Wang, M., Chang, Y., Zhang, F., Ban, Z., Tang, R., Gan, Q., Wu, S., Guo, Y., Zhang, Q., Wang, F., Zhao, L., Jing, Y., Qian, W., Wang, G., Guo, W., Yang, C., 2018. The lysine catabolite saccharopine impairs development by disrupting mitochondrial homeostasis. J. Cell Biol. 218, 580–597. https://doi.org/10.1083/jcb.201807204.
Zhou, Y., Eid, T., Hassel, B., Danbolt, N.C., 2020. Novel aspects of glutamine synthetase in ammonia homeostasis. Neurochem. Int. 140, 104809. https://doi.org/10.1016/j.neuint.2020.104809.
Zuberi, Z., Eeza, N.H.M., Matysik, J., Berry, P.J., Alia, A., 2019. NMR-based metabolic profiles of intact zebrafish embryos exposed to aflatoxin B1 recapitulates hepatotoxicity and supports possible neurotoxicity. Toxins 11. https://doi.org/10.3390/toxins11050258.